NCBI Nucleotide

PubMed Nucleotide Protein Genome Structure PopSet Taxonomy OMIM Boo

Search Nucleotide for Go Clear

Limits Preview/Index History Clipboard Details

Display default Save Text Add to Clipboard

☐ **1:** NM_031361. Homo sapiens coll... [gi:14165451]

MapView, Related Sequences, OMIM, Protein, PubMed, SNP, Taxonomy, LinkOut

```
LOCUS       COL4A3BP                2311 bp    mRNA    linear   PRI 31-JUL-2002
DEFINITION  Homo sapiens collagen, type IV, alpha 3 (Goodpasture antigen)
            binding protein (COL4A3BP), transcript variant 2, mRNA.
ACCESSION   NM_031361
VERSION     NM_031361.1  GI:14165451
KEYWORDS    .
SOURCE      human.
  ORGANISM  Homo sapiens
            Eukaryota; Metazoa; Chordata; Craniata; Vertebrata; Euteleostomi;
            Mammalia; Eutheria; Primates; Catarrhini; Hominidae; Homo.
REFERENCE   1  (bases 1 to 2311)
  AUTHORS   Kalluri,R.
  TITLE     Goodpasture syndrome
  JOURNAL   Kidney Int. 55 (3), 1120-1122 (1999)
  MEDLINE   99152238
   PUBMED   10027952
REFERENCE   2  (bases 1 to 2311)
  AUTHORS   Raya,A., Revert,F., Navarro,S. and Saus,J.
  TITLE     Characterization of a novel type of serine/threonine kinase that
            specifically phosphorylates the human goodpasture antigen
  JOURNAL   J. Biol. Chem. 274 (18), 12642-12649 (1999)
  MEDLINE   99230287
   PUBMED   10212244
REFERENCE   3  (bases 1 to 2311)
  AUTHORS   Raya,A., Revert-Ros,F., Martinez-Martinez,P., Navarro,S.,
            Rosello,E., Vieites,B., Granero,F., Forteza,J. and Saus,J.
  TITLE     Goodpasture antigen-binding protein, the kinase that phosphorylates
            the goodpasture antigen, is an alternatively spliced variant
            implicated in autoimmune pathogenesis
  JOURNAL   J. Biol. Chem. 275 (51), 40392-40399 (2000)
  MEDLINE   20568301
   PUBMED   11007769
COMMENT     REVIEWED REFSEQ: This record has been curated by NCBI staff. The
            reference sequence was derived from AF232930.1 and AF136450.1.
            Summary: This gene encodes a kinase that specifically
            phosphorylates the N-terminal region of the non-collagenous domain
            of the alpha 3 chain of type IV collagen, known as the Goodpasture
            antigen. Goodpasture disease is the result of an autoimmune
            response directed at this antigen. Two transcripts exist for this
            gene.
            Transcript Variant: This variant (2) lacks an exon that encodes a
            26 amino acid region with a serine-rich motif, as compared to
            variant 1. The absence of this motif results in a less active
            protein.
FEATURES             Location/Qualifiers
```

```
source          1..2311
                /organism="Homo sapiens"
                /db_xref="taxon:9606"
                /chromosome="5"
                /map="5q13.1"
gene            1..2311
                /gene="COL4A3BP"
                /note="GPBP"
                /db_xref="LocusID:10087"
                /db_xref="MIM:604677"
CDS             409..2205
                /gene="COL4A3BP"
                /EC_number="2.7.1.37"
                /note="isoform 2 is encoded by transcript variant 2;
                goodpasture antigen-binding protein"
                /codon_start=1
                /product="alpha 3 type IV collagen binding protein isoform
                2"
                /protein_id="NP_112729.1"
                /db_xref="GI:14165452"
                /db_xref="LocusID:10087"
                /db_xref="MIM:604677"
                /translation="MSDNQSWNSSGSEEDPETESGPPVERCGVLSKWTNYIHGWQDRW
                VVLKNNALSYYKSEDETEYGCRGSICLSKAVITPHDFDECRFDISVNDSVWYLRAQDP
                DHRQQWIDAIEQHKTESGYGSESSLRRHGSMVSLVSGASGYSATSTSSFKKGHSLREK
                LAEMETFRDILCRQVDTLQKYFDACADAVSKDELQRDKVVEDDEDDFPTTRSDGDFLH
                STNGNKEKLFPHVTPKGINGIDFKGEAITFKATTAGILATLSHCIELMVKREDSWQKR
                LDKETEKKRRTEEAYKNAMTELKKKSHFGGPDYEEGPNSLINEEEFFDAVEAALDRQD
                KIEEQSQSEKVRLHWPTSLPSGDAFSSVGTHRFVQKVEEMVQNHMTYSLQDVGGDANW
                QLVVEEGEMKVYRREVEENGIVLDPLKATHAVKGVTGHEVCNYFWNVDVRNDWETTIE
                NFHVVETLADNAIIIYQTHKRVWPASQRDVLYLSVIRKIPALTENDPETWIVCNFSVD
                HDSAPLNNRCVRAKINVAMICQTLVSPPEGNQEISRDNILCKITYVANVNPGGWAPAS
                VLRAVAKREYPKFLKRFTSYVQEKTAGKPILF"
misc_feature    478..756
                /gene="COL4A3BP"
                /note="Region: pfam00169, PH domain. PH stands for
                pleckstrin homology"
misc_feature    478..753
                /gene="COL4A3BP"
                /note="Region: smart00233, PH, Pleckstrin homology domain.
                Domain commonly found in eukaryotic signalling proteins.
                The domain family possesses multiple functions including
                the abilities to bind inositol phosphates, and various
                proteins. PH domains have been found to possess inserted
                domains (such as in PLC gamma, syntrophins) and to be
                inserted within other domains. Mutations in Brutons
                tyrosine kinase (Btk) within its PH domain cause X-linked
                agammaglobulinaemia (XLA) in patients. Point mutations
                cluster into the positively charged end of the molecule
                around the predicted binding site for phosphatidylinositol
                lipids"
misc_feature    1567..2184
                /gene="COL4A3BP"
                /note="Region: pfam01852, START domain"
misc_feature    1570..2175
                /gene="COL4A3BP"
                /note="Region: smart00234, START, in StAR and
                phosphatidylcholine transfer protein; putative
                lipid-binding domain in StAR and phosphatidylcholine
                transfer protein"
```

```
     misc_feature    1518^1519
                     /gene="COL4A3BP"
                     /note="Region: exon removed in transcript variant 2"
     variation       complement(1701)
                     /allele="C"
                     /allele="T"
                     /db_xref="dbSNP:698912"
BASE COUNT      653 a    472 c    592 g    594 t
ORIGIN
        1 gcaggaagat ggcggcggta gcggaggtgt gagtggacgc gggactcagc ggccggattt
       61 tctcttccct tcttttccct tttccttccc tatttgaaat tggcatcgag ggggctaagt
      121 tcgggtggca gcgccgggcg caacgcaggg gtcacggcga cggcggcggc ggctgacggc
      181 tggaagggta ggcttcattc accgctcgtc ctccttcctc gctccgctcg gtgtcaggcg
      241 cggcggcggc gcggcgggcg gacttcgtcc ctcctcctgc tccccccac accggagcgg
      301 gcactcttcg cttcgccatc ccccgaccct tcaccccgag gactgggcgc ctcctccggc
      361 gcagctgagg gagcgggggc cggtctcctg ctcggttgtc gagcctccat gtcggataat
      421 cagagctgga actcgtcggg ctcggaggag gatccagaga cggagtctgg gccgcctgtg
      481 gagcgctgcg ggtcctcag taagtggaca aactacattc atgggtggca ggatcgttgg
      541 gtagttttga aaaataatgc tctgagttac tacaaatctg aagatgaaac agagtatggc
      601 tgcagaggat ccatctgtct tagcaaggct gtcatcacac ctcacgattt tgatgaatgt
      661 cgatttgata ttagtgtaaa tgatagtgtt tggtatcttc gtgctcagga tccagatcat
      721 agacagcaat ggatagatgc cattgaacag cacaagactg aatctggata tggatctgaa
      781 tccagcttgc gtcgacatgg ctcaatggtg tccctggtgt ctggagcaag tggctactct
      841 gcaacatcca cctcttcatt caagaaaggc cacagtttac gtgagaagtt ggctgaaatg
      901 gaaacattta gagacatctt atgtagacaa gttgacacgc tacagaagta ctttgatgcc
      961 tgtgctgatg ctgtctctaa ggatgaactt caaagggata aagtggtaga agatgatgaa
     1021 gatgactttc ctacaacgcg ttctgatggt gacttcttgc atagtaccaa cggcaataaa
     1081 gaaaagttat ttccacatgt gacaccaaaa ggaattaatg gtatagactt taaaggggaa
     1141 gcgataactt ttaaagcaac tactgctgga atccttgcaa cactttctca ttgtattgaa
     1201 ctaatggtta aacgtgagga cagctggcag aagagactgg ataaggaaac tgagaagaaa
     1261 agaagaacag aggaagcata taaaaatgca atgacagaac ttaagaaaaa atcccacttt
     1321 ggaggaccag attatgaaga aggccctaac agtctgatta atgaagaaga gttctttgat
     1381 gctgttgaag ctgctcttga cagacaagat aaaatagaag aacagtcaca gagtgaaaag
     1441 gtgagattac attggcctac atccttgccc tctggagatg ccttttcttc tgtggggaca
     1501 catagatttg tccaaaaggt tgaagagatg gtgcagaacc acatgactta ctcattacag
     1561 gatgtaggcg gagatgccaa ttggcagttg gttgtagaag aaggagaaat gaaggtatac
     1621 agaagagaag tagaagaaaa tgggattgtt ctggatcctt taaaagctac ccatgcagtt
     1681 aaaggcgtca caggacatga agtctgcaat tatttctgga atgttgacgt tcgcaatgac
     1741 tgggaaacaa ctatagaaaa ctttcatgtg gtggaaacat tagctgataa tgcaatcatc
     1801 atttatcaaa cacacaagag ggtgtggcct gcttctcagc gagacgtatt atatctttct
     1861 gtcattcgaa agataccagc cttgactgaa aatgaccctg aaacttggat agtttgtaat
     1921 ttttctgtgg atcatgacag tgctcctcta aacaaccgat gtgtccgtgc caaaataaat
     1981 gttgctatga tttgtcaaac cttggtaagc ccaccagagg gaaaccagga aattagcagg
     2041 gacaacattc tatgcaagat tacatatgta gctaatgtga accctggagg atgggcacca
     2101 gcctcagtgt taagggcagt ggcaaagcga gagtatccta aatttctaaa acgttttact
     2161 tcttacgtcc aagaaaaaac tgcaggaaag cctattttgt tctagtatta acaggtacta
     2221 gaagatatgt tttatctttt tttaacttta tttgactaat atgactgtca atactaaaat
     2281 ttagttgttg aaagtattta ctatgttttt t
//
```

Revised: July 5, 2002.

Schiff base complex shows that Wat[21] is equivalent to Wat[29]. Also in the native structure, a water molecule is found in the identical position (within 0.5 Å of Wat[29] of the carbinolamine). Wat[72] in the Schiff base complex could correspond to the water molecule derived from protonation of the hydroxyl group of the carbinolamine.

25. Known class I structures used for comparison were KDPG aldolase in complex with pyruvate [Protein Data Bank (PDB) code 1EUA] (17), human muscle fructose 1,6-bisphosphate aldolase (PDB code 4ALD) (19), rabbit muscle 1,6-bisphosphate fructose aldolase (PDB code 1ADO) (20), and transaldolase B (PDB code 1UCW) (21).
26. This mutant crystallized under the same conditions as the wild type, and the substrate soak was repeated as reported in Table 1.
27. This observation was also made for the rabbit aldolase A, where the $Lys^{146} \rightarrow Arg^{146}$ mutant retained the ability to form the Schiff base intermediate (43).
28. F. H. Westheimer, D. E. Schmidt Jr., *Biochemistry* **10**, 1249 (1971).
29. F. H. Westheimer, *Tetrahedron* **51**, 3 (1995).
30. Experimental conditions for the pH activity profile were as follows: 25 mM buffer solutions of sodium formate (pH 3.5, 3.0, and 4.0); sodium acetate (pH 4.5, 5.0, and 5.5); MES (pH 5.5, 6.0, and 6.5); MOPS (pH 6.5, 7.0, and 7.5); tetraethylammonium-chloride (TEA-HCl) (pH 7.5, 8.0, and 8.5); CAPSO (pH 8.5, 9.0, and 9.5), and CAPS (pH 10, 10.5, and 11.0). V_{max} was measured from pH 4 to 10 in the retroaldol direction with 3 mM DRP in 50 mM (pH 7.5) TEA-HCl buffer in the presence of 0.3 mM reduced nicotinamide adenine dinucleotide (NADH) using a glyceraldehyde 3-phosphate dehydrogenase/triosephosphate isomerase (GPD/TPI)-coupled (5.3 U/ml, Sigma G-1881) enzyme system at 25°C by observing the rate of decrease of NADH concentration as monitored at 340 nm (44).
31. In rabbit aldolase A, the equivalent Lys^{146} residue has been implicated as being involved in cleavage and condensation of the C3–C4 bond of fructose 1,6-bisphosphate (45), in addition to lowering the pK_a of Lys^{229}.
32. All solvent-accessible surface areas were calculated with the program MS (46) with a 1.4 Å probe sphere and standard atomic radii (47).
33. Experimental conditions for the Schiff base trapping experiment were as follows: DERA (1 mg/ml) was incubated with 5 mM acetaldehyde in 20 mM TEA-HCl, 50 mM NaCl, and 2 mM $CaCl_2$ (pH 7.4) at 22°C for 10 min. Fifty mM $NaBH_4$ was added, and incubation continued for 12 hours. Samples were dialyzed against dH_2O and then purified by high-performance liquid chromatography on a C18 column before analysis by electrospray ionization mass spectrometry (with a Perkin Elmer API III Sciex triple quadrupole). Observed masses agreed within ±4 daltons to theoretical values.
34. A. Heine, J. G. Luz, C.-H. Wong, I. A. Wilson, in preparation.
35. J. A. Littlechild, H. C. Watson, *Trends Biochem. Sci.* **18**, 36 (1993).
36. The activity of the class I aldolase from halophilic archaebacterium *Haloarcula vallismortis* was not affected by carboxypeptidase digestion (48).
37. The model was constructed with Molecular Simulations Insight 2000. Setup was as described (49). The CVFF force field provided in the Discover module of Insightll was used.
38. C. F. Barbas III, thesis, Texas A&M University, College Station, TX (1989).
39. Experimental conditions for deuteropropanal synthesis and the DERA exchange experiment were as follows: (*R*)-2-deuteropropanol was synthesized from (*S*)-(+)-1,2-propanediol as described in (50) with minor modification. ^{1}H NMR ($CDCl_3$, 500 MHz): 3.62 (d, J = 6.97 Hz, 2H), 1.60 to 1.55 (m, 1H), 0.91 (d, J = 7.34 Hz, 3H). ^{13}C NMR ($CDCl_3$, 125 MHz): 64.58, 24.79 (t, J = 20 Hz), 9.91. (*R*)-2-deuteropropanol: $[\alpha]_D$ = +1.11°, ($CDCl_3$, c = 0.18); lit. +0.06°, (neat). (*S*)-2-deuteropropanol was prepared analogously: $[\alpha]_D$ = −0.05° ($CDCl_3$, c = 1.8); lit. −0.06° (neat). In an NMR tube, (*R*)- or (*S*)-2-deuteropropanol was incubated at 0.4 mM in 100 mM TEA-HCl buffer made up with D_2O together with 8 mM pyruvic acid, 1 mM NAD^+, yeast alcohol dehydrogenase (0.25 mg/ml) (82.5 U), and L-lactic dehydrogenase (0.25 mg/ml) (214.5 U), pH in D_2O (pD) = 7.1. After the oxidation of deuteropropanol to deuteropropanal was deemed substantially complete by the appearance of the aldehyde C3 resonance by ^{1}H NMR (D_2O, 500 MHz): 1.08 (d, J = 7.34 Hz, 3H), then 0.5 mg/ml (50 U) wild-type DERA was added. For (*R*)-2-deuteropropanal, this resonance collapses to a singlet 1.04 (s, 3H) after 3 hours, whereas for (*S*)-2-deuteropropanal it remains unchanged.
40. L. Chen, D. P. Dumas, C.-H. Wong, *J. Am. Chem. Soc.* **114**, 741 (1992).
41. T. M. Larsen, M. M. Benning, L. Rayment, G. H. Reed, *Biochemistry* **37**, 6247 (1998).
42. R. R. Copley, G. J. Barton, *J. Mol. Biol.* **242**, 321 (1994).
43. A. J. Morris, R. C. Davenport, D. R. Tolan, *Prot. Eng.* **9**, 61 (1996).
44. P. C. Nicholas, *Biochem. Soc. Trans.* **16**, 752 (1988).
45. A. J. Morris, D. R. Tolan, *Biochemistry* **33**, 12291 (1994).
46. M. L. Connolly, *J. Appl. Crystallogr.* **16**, 439 (1983).
47. S. Sheriff, *Immunomethods* **3**, 191 (1993).
48. G. Krishnan, W. Altekar, *Eur. J. Biochem.* **195**, 343 (1991).
49. G. DeSantis, J. B. Jones, *J. Am. Chem. Soc.* **120**, 8582 (1998).
50. M. M. Green, J. M. Moldowan, J. G. McGrew II, *J. Org. Chem.* **39**, 2166 (1974).
51. Z. Otwinowski, W. Minor, *Methods Enzymol.* **276A**, 307 (1997).
52. A. T. Brünger *et al.*, *Acta Crystallogr. D* **54**, 905 (1998).
53. G. M. Sheldrick, T. R. Schneider, *Methods Enzymol.* **277B**, 319 (1997).
54. T. A. Jones, J. Y. Zou, S. W. Cowan, M. Kjeldgaard, *Acta Crystallogr. A* **47**, 110 (1991).
55. H. Kim, U. Certa, H. Dobeli, P. Jakob, W. G. Hol, *Biochemistry* **37**, 4388 (1998).
56. J. Sygusch, D. Beaudry, M. Allaire, *Proc. Natl. Acad. Sci. U.S.A.* **84**, 7846 (1987).
57. R. A. Laskowski, M. W. MacArthur, D. S. Moss, J. M. Thornton, *J. Appl. Crystallogr.* **26**, 283 (1993).
58. P. C. Nicholas, *Biochem. Soc. Trans.* **16**, 752 (1988).
59. Experimental conditions for propanal exchange with DERA mutants were as follows: In an NMR tube, propropanal was incubated at 200 mM in 100 mM TEA-HCl buffer made up with D_2O (pD = 7.1) and DERA (2 mg/ml) was added (50 U for wild-type DERA). Samples were analyzed by ^{1}H NMR (D_2O, 250 MHz). For wild-type DERA, the C3-aldehyde triplet resonance 1.03 (t, J = 7.01 Hz, 3H) collapses to a doublet 1.02 (d, J = 7.3 Hz, 3H).
60. P. J. Kraulis, *J. Appl. Crystallogr.* **24**, 946 (1991).
61. E. A. Merritt, D. J. Bacon, *Methods Enzymol.* **277**, 505 (1997).
62. We gratefully acknowledge helpful discussions with F. Huang, S. Fong, L. Lee, T. Tolbert, P. Sears, W. W. Cleland, G. M. Sheldrick, J. H. Naismith, and R. A. Lerner. Supported by NIH grants GM44154 (C.H.W.) and CA27489 (I.A.W.), a Natural Science and Engineering Research Council of Canada postdoctoral fellowship (G.D.), and a UNCF-Merck Science Initiative fellowship (M.M.). We thank the Stanford Synchrotron Radiation Laboratory staff of beamline 9-2, X. Dai, and S. E. Greasley for help with data collection and processing, and M. Elsliger for computational assistance. This is publication 14200-MB from the Scripps Research Institute. The coordinates have been deposited in the PDB with access codes 1JCL (wild-type DERA) and 1JCJ (K201L mutant of DERA) and are available immediately from aheine@scripps.edu.

19 June 2001; accepted 2 August 2001

Carboxyl-Terminal Modulator Protein (CTMP), a Negative Regulator of PKB/Akt and v-Akt at the Plasma Membrane

Sauveur-Michel Maira,[1] Ivana Galetic,[1] Derek P. Brazil,[1] Stefanie Kaech,[1*] Evan Ingley,[1†] Marcus Thelen,[2] Brian A. Hemmings[1‡]

The PKB (protein kinase B, also called Akt) family of protein kinases plays a key role in insulin signaling, cellular survival, and transformation. PKB is activated by phosphorylation on residues threonine 308, by the protein kinase PDK1, and Serine 473, by a putative serine 473 kinase. Several protein binding partners for PKB have been identified. Here, we describe a protein partner for PKBα termed CTMP, or carboxyl-terminal modulator protein, that binds specifically to the carboxyl-terminal regulatory domain of PKBα at the plasma membrane. Binding of CTMP reduces the activity of PKBα by inhibiting phosphorylation on serine 473 and threonine 308. Moreover, CTMP expression reverts the phenotype of v-*Akt*–transformed cells examined under a number of criteria including cell morphology, growth rate, and in vivo tumorigenesis. These findings identify CTMP as a negative regulatory component of the pathway controlling PKB activity.

PKB is a major downstream target of receptor tyrosine kinases that signal via the phosphatidylinositol 3-kinase (PI 3-kinase). PKB mediates a wide variety of biological responses to insulin and insulin-like growth factor 1 (IGF-1) and other growth factors (*1–2*). Upon cell stimulation, the kinase is translocated to the plasma membrane, where it is phosphorylated on two amino acids, Thr^{308} in the catalytic domain and Ser^{473} in the COOH-

ıal regulatory domain (*3–8*). To date, ɔroteins have been shown to physically ːt with PKB (*9–11*).

identify new proteins that interact with a HeLa cell cDNA library was screened ast two-hybrid analysis, with the kinase in plus the COOH-terminal regulatory do- of PKBα as bait. From 1.5 × 10[6] primary ormants screened, seven identical clones identified. This cDNA encoded a protein pecifically interacted with PKBα, as dem- ated by activation of the reporters for his- : auxotrophy and lacZ activity [Web fig. 1, d B (*12*)], and in a mammalian cell two- id assay (*13*). This interaction was observed with constructs containing the COOH-ter- l regulatory domain of PKBα, encompass- ımino acids 411 to 480 [Web fig. 1, C and 2)]. Sequence analysis revealed the pres- : of an open reading frame encoding a ein of 240 amino acids with a predicted molecular mass of 27 kD that we termed COOH-terminal modulator protein, or CTMP (Fig. 1A). The cDNA contains the unusual feature of an Alu cassette at its 3′ end, a sequence usually found in intronic DNA. Database screening of mouse expressed sequence tags revealed a protein of 230 amino acids with a similar sequence (79% identity) that may be the mouse homolog of CTMP (Fig. 1A). The mRNA for human CTMP was detected predominantly in skeletal muscle, testis, uterus, brain, and kidney, with lower levels observed in heart, liver, and lung [Web fig. 2A (*12*)]. The presence of multiple bands after reverse transcription–polymerase chain reaction (RT-PCR) strongly suggested that the gene for CTMP undergoes alternate splicing in some tissues, generating multiple RNA transcripts [Web fig. 3, A and B (*12*)]. Endogenous CTMP protein was detected with an antibody (*14*) specific for human CTMP in extracts from HeLa and human embryonic kidney (HEK) 293 cells, with weaker expression found in COS-1 cells [Web fig. 2B (*12*)]. Weaker CTMP expression was seen in the human SJRH30 rhabdomyosarcoma cell line, and no signal was detected in the rat H9C2 myocardium cell line. These data were confirmed by blotting with a second antibody against CTMP (*13*). CTMP migrated with apparent molecular masses of 22 to 26 kD in the different cell lines, possibly owing to post-translational modification (see below).

When HeLa cell extracts were subjected to centrifugation into cytosolic (S100) and membrane (P100) fractions, endogenous CTMP was predominantly detected in the P100 fraction [Web fig. 2C (*12*)]. CTMP expression was detected in a range of different human cell lines (*15*), most notably in a glioblastoma cell line (LN229, Fig. 1C). Again, two molecular species corresponding to CTMP were observed in LN229 cells, and these forms appeared to be differentially localized to the membrane and cytosolic fractions of these cells (Fig. 1D). Immunofluorescence analysis demonstrated that endogenous PKB and CTMP colocalized at the plasma membrane (Fig. 1E). Endogenous complexes of CTMP and PKB were also detected in the P100 fraction of these cells by Western blotting (*16*). Immunolocalization of green fluorescent protein (GFP)–CTMP fusion protein indicated that CTMP associated with intracellular structures similar to membrane ruffles (Fig. 1B), whereas staining of the GFP control protein was detected in all cellular compartments. Time-lapse cine-microscopy of moving NIH 3T3 cells expressing GFP-CTMP revealed that the fusion protein was predominantly localized to the leading edge of the moving cells, decorating the rapidly moving membrane ruffles [Web fig. 4 (*12*)].

Western blotting of lysates from a control cell line stably expressing CTMP indicated that

ːdrich Miescher Institute, Post Office Box 2543, 4002 Basel, Switzerland. [2]Institute for Research in nedicine, CH-6500 Bellinzona, Switzerland.

ːsent address: Center for Research in Occupational Environmental Toxicology, Oregon Health Sci- ː University, Portland, OR 97201–3098, USA. ːsent address: Department of Biochemistry, Royal ːh Hospital, GPO Box X2213, Western Australia ı1, Australia.

ı whom correspondence should be addressed. E- il: hemmings@fmi.ch

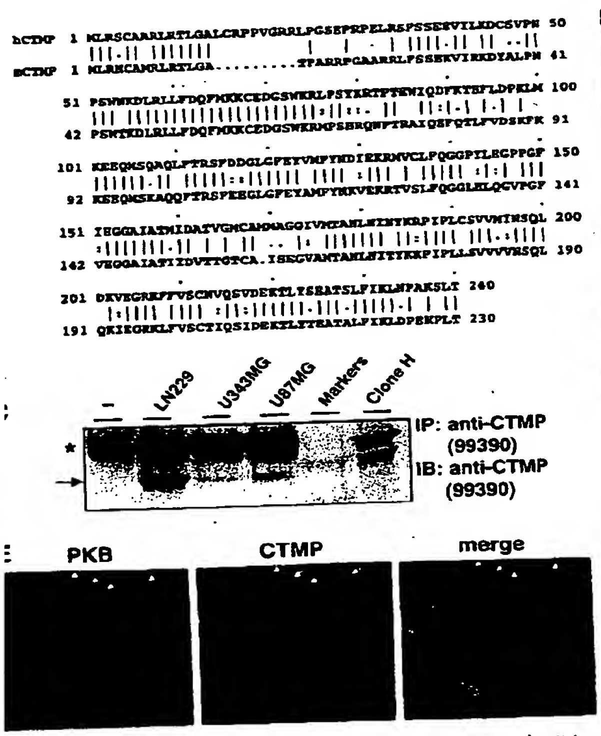

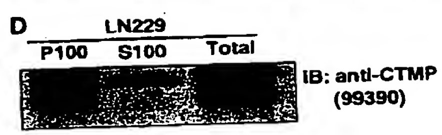

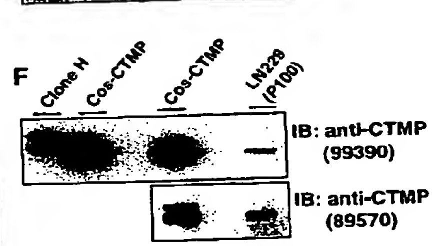

Fig. 1. Structure and localization of human CTMP. (**A**) Alignment of deduced amino acid sequences from human (accession number AJ313515) and mouse CTMP. (**B**) NIH 3T3 cells were transfected with 5 μg of expression vectors for GFP (pGFP, left panel) or GFP-CTMP (pGFP-CTMP, right panel) (*29*). GFP fluorescence was then analyzed in living cells using confocal microscopy (*30*). The arrows indicate areas of high fluorescence intensity at membrane ruffles. (**C**) CTMP expression in glioblastoma cell lines was assessed by immunoprecipitation followed by immunoblotting with the same antibody against CTMP (99390). The position of CTMP is indicated by an arrow. Clone H is a cell-line stably expressing Flag-CTMP (see Fig. 5). The asterisk represents the IgG light chain. (**D**) Detection of endogenous CTMP protein by Western blotting of equivalent amounts (50 μg) of cytosolic (S100), membrane (P100) fractions (*31*) or total cell lysate (Total) from LN229 cells. (**E**) To determine the cellular distribution of endogenous PKBα and CTMP proteins, LN229 cells were fixed with 4% paraformaldehyde and incubated with PKB mAb (*32*), followed by staining with protein A/G coupled to FITC (green, PKB panel), or with the polyclonal CTMP antibody 99390 followed by staining with rhodamine-conjugated rabbit antibody (red, CTMP panel). Slides were analyzed by confocal microscopy, and the pictures represent the central section of the x-y plane. Areas of colocalization of CTMP and PKB at the membrane ruffles are visualized in yellow (merge panel) and are indicated by arrows. (**F**) CTMP from pHook2-CTMP transfected COS-1 cells (*29*), clone H cell extracts, or P100 fraction from LN229 cells was detected with CTMP antibodies 99390 and 89570 (*14*).

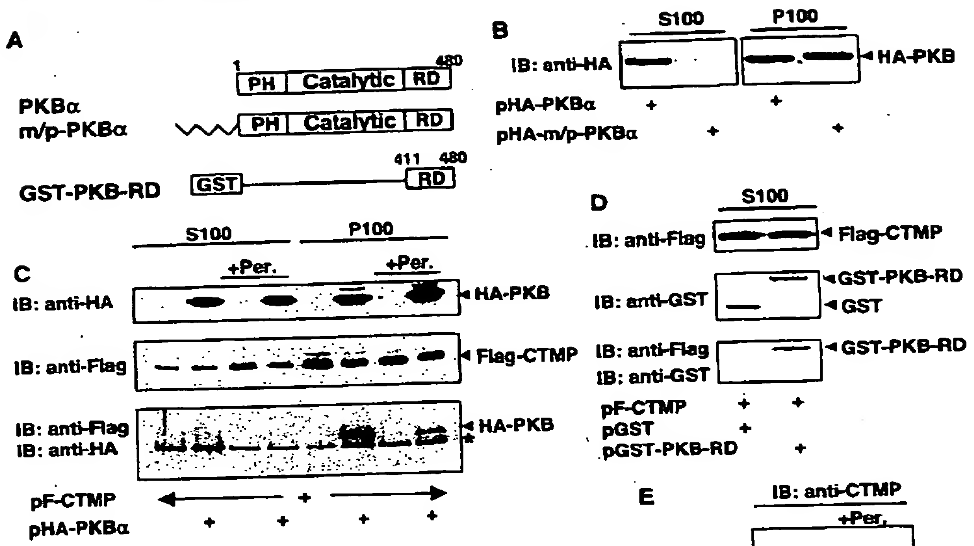

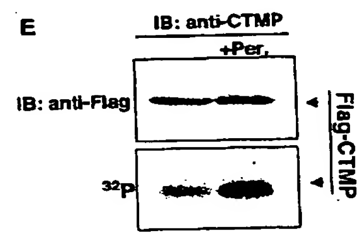

ig. 2. Interaction of CTMP and PKBα in quiesent cells, and phosphorylation following stimilation. (A) Schematic diagram of recombinant proteins used in these experiments (33). (B) COS-1 cells were transfected with 7.5 μg of the ndicated PKB expression vectors, lysed, and ractionated (31). Soluble (S100) and particuate (P100) fractions were analyzed by Western blotting using the HA mAb 12CA5 (14). (C) COS-1 cells were transfected with 7.5 μg of the ndicated PKB (33) and CTMP (29) expression vectors. After serum starvation (24 hours) and stimulation with 100 μM pervanadate (15 min at 37°C, +Per.), cells were lysed and fractionated. Immunoprecipitations were performed from S100 and P100 fractions using an antibody against Flag (14). PKBα expression was analyzed using an HA antibody (upper panel), CTMP expression was analyzed using Flag antiserum (middle panel), and CTMP-bound PKBα was detected using an HA antibody (bottom panel). The asterisk represents the IgG heavy chain. (D) COS-1 cells were transfected with 7.5 μg of pF-CTMP and with pGST or pGST-PKB-RD. Cells were lysed and fractionated as in Fig. 2B, and immunoprecipitations were performed from the S100 fractions with a Flag antibody. Association of GST-PKB-RD with CTMP was analyzed using a GST antibody (14). (E) Cells stably expressing Flag-CTMP were labeled in vivo with [^{32}P] orthophosphate (34). After immunoprecipitation, phosphorylated Flag-CTMP was revealed by SDS–polyacrylamide gel electrophoresis (SDS-PAGE) and Western-blotting, followed by autoradiography of the membrane (bottom panel). Expression level of Flag-CTMP was revealed by immunoblotting of the membrane with antibody against Flag (upper panel).

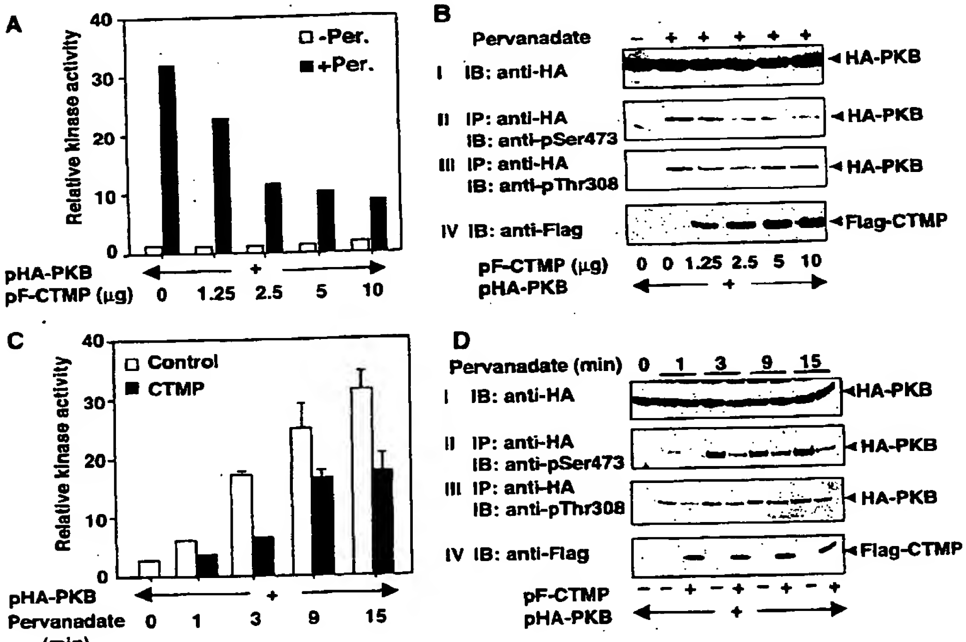

Fig. 3. CTMP inhibits PKBα activity by preventing its phosphorylation by upstream kinases. (A) COS-1 cells were cotransfected with an HA-PKB expression vector (2.5 μg) and with the indicated amount of pF-CTMP. Cells were serum-starved (24 hours), and stimulated with vehicle control (white bars) or 100 μM pervanadate (black bars) for 10 min at 37°C. Cells were then lysed and analyzed for PKB kinase activity as described (35). (B) The phosphorylation status of PKBα was investigated by using antibodies against pSer^{473} (panel II) and Thr^{308} (panel III) (14). Expressed PKBα (panel I) and CTMP (panel IV) proteins were detected with the indicated antibodies (14). (C) COS-1 cells were transfected with an HA-PKBα expression vector (2.5 μg) together with 5 μg control vector (control, white bars) or 5 μg pF-CTMP (CTMP, black bars). Serum-starved cells (24 hours) were then stimulated with 100 μM pervanadate at 37°C for the indicated times, lysed, and processed for immune-kinase assay (35). (D) Immunoprecipitations from COS-1 cells transfected with the indicated constructs were analyzed for phosphorylation on PKBα residues Ser^{473} or Thr^{308} as described in Fig. 3B.

two forms of CTMP exist in these cells (Fig. 1, C and F; also see Fig. 5 for details). Transfection of CTMP without an epitope tag also produced two species of CTMP, suggesting that this protein undergoes posttranslational modifications such as phosphorylation in cells (Fig. 1F; also see Fig. 2E). It is interesting that the lower of the two CTMP forms in transfected cells comigrated with endogenous CTMP detected in the P100 fraction of LN229 cells (Fig. 1D). This further suggests that CTMP localization in the cell may be regulated by posttranslational modifications such as phosphorylation.

To further explore the biological relevance of the PKBα-CTMP complex, this interaction was analyzed in mammalian cells by immunoprecipitation. In cell extracts from transfected COS-1 cells lysed in buffer containing 1% NP-40 (v/v), CTMP formed a complex with a COOH-terminal regulatory domain mutant of PKBα (GST-PKB-RD, Fig. 2A), but not with full-length PKBα. One interpretation of this result is that binding of CTMP and PKBα may require intact plasma membrane structures, because both proteins have the ability to localize at the plasma membrane [(17) and Fig. 1B]. We therefore lysed transfected COS-1 cells in Hepes/sucrose buffer, facilitating the preparation of cytosolic (S100) and membrane (P100) fractions for immunoprecipitation. The efficiency of the fractionation was confirmed by transfection of a membrane-targeted PKB (m/p-PKB), a construct containing sites for myristoylation and palmitoylation of PKB that result in constitutive membrane anchoring [(17) and Fig. 2A]. The m/p-PKB protein was exclusively localized in the P100 fraction of lysed COS-1 cells (Fig. 2B). In contrast, wild-type PKBα

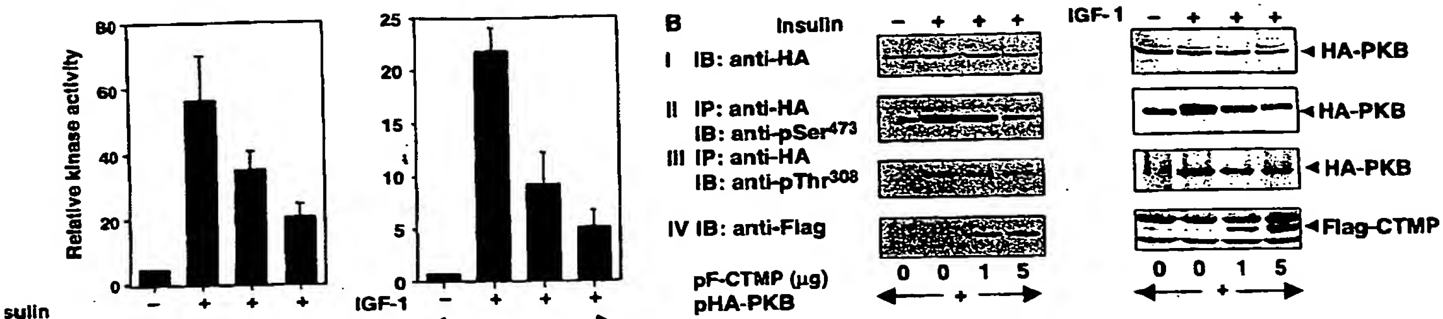

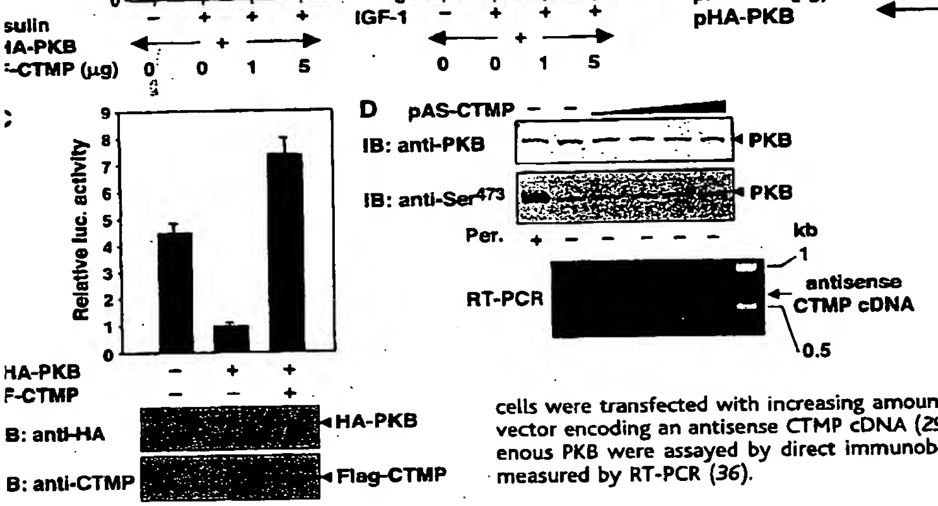

Fig. 4. Effect of CTMP on PKBα signaling. **(A)** HEK293 cells transfected with expression vectors for HA-PKBα (1 μg) and pF-CTMP (amounts indicated) were serum-starved (24 hours) and stimulated with either insulin (100 nM, 15 min) or IGF-1 (50 nM, 10 min) at 37°C. Cells were then processed for immune-kinase assay (*35*). **(B)** Phosphorylation status of PKBα residues Ser[473] and Thr[308] was investigated as described in Fig. 3B. **(C)** HEK293 cells were transfected with 200 ng of the p-*fos*–*luc* reporter gene together with pHA-PKB (200 ng) and pF-CTMP (1 μg) where indicated. Luciferase assays were performed 48 hours after transfection as described by the manufacturer (Promega luciferase assay kit). **(D)** HEK293 cells were transfected with increasing amounts of pAS-CTMP (1, 2, 4, and 10 μg), an expression vector encoding an antisense CTMP cDNA (*29*). Expression and Ser[473] phosphorylation of endogenous PKB were assayed by direct immunoblotting (*14*). The amounts of antisense cDNA were measured by RT-PCR (*36*).

ras equally distributed between the membrane nd cytosolic fractions. Association of PKBα nd CTMP was examined by cotransfection of :OS-1 cells with constructs encoding epitope-ıgged versions of both proteins [hemaggluti-in-tagged (HA)-PKBα and Flag-CTMP, Fig. C]. Both PKBα (upper panel) and CTMP middle panel) were detected in cytosolic S100) and membrane (P100) fractions (Fig. C). In addition, PKBα was observed in CTMP mmunoprecipitates from membrane, but not ytosolic fractions (Fig. 2C, bottom panel). 'reatment of COS-1 cells with pervanadate, an ahibitor of protein tyrosine phosphatases that otently activates PKB (*18*), disrupted the 'KBα-CTMP interaction in the membrane raction (Fig. 2C, bottom panel). These data onfirm that PKBα interacts with CTMP in uiescent or unstimulated cells and that activa-ion of PKBα with pervanadate perturbs this nteraction. In contrast to full-length PKBα, a runcation mutant containing the COOH-termi-ıal regulatory domain of PKBα (GST-PKB-ID, Fig. 2A) was detected in CTMP immuno-recipitates from cytosolic fractions of COS-1 :ells (Fig. 2D). These observations suggest that ı region of PKBα not present in the GST-PKB-ID construct inhibits the binding of CTMP to :ytosolic PKBα. Alternately, other proteins nay be involved in the formation of PKB-CTMP complexes. These data further support he hypothesis that binding of full-length PKBα and CTMP occurs only at the plasma nembrane.

To explore a potential mechanism for the inhibitory effect of pervanadate on PKBα-CTMP complexes, we monitored phosphorylation of CTMP during PKB activation. In vivo labeling of cells stably expressing Flag-CTMP with [^{32}P]orthophosphate demonstrated a fourfold increase in CTMP phosphorylation after pervanadate treatment (Fig. 2E), supporting the idea that CTMP is regulated at the posttranslational level by as-yet-unidentified protein kinases.

Activation of PKBα occurs via phosphorylation of Thr[308] in the activation loop of the kinase domain and of Ser[473] in the COOH-terminal regulatory domain (*5*). To test the influence of CTMP binding on activation of PKBα, we assayed kinase activity in immune complexes from transfected COS-1 cells treated with pervanadate. Pervanadate-stimulated PKBα activity was decreased in a manner dependent on the amount of transfected CTMP (Fig. 3A). Therefore, CTMP binding appears to have an inhibitory effect on PKB. Increased CTMP expression led to decreased phosphorylation on both Ser[473] and Thr[308] residues of PKBα, most notably on Ser[473] (Fig. 3B). Especially at late time points, kinase activity of PKBα was stimulated by pervanadate, despite the presence of CTMP (Fig. 3C). This increase in activity over time was reflected in increases in phosphorylation of PKBα residues Ser[473] and Thr[308] in the presence or absence of CTMP (Fig. 3D). These results show that binding of CTMP to PKBα inhibits, but does not completely abolish, pervanadate-stimulated phosphorylation of the key amino acids necessary for kinase activity of PKBα.

To determine the effect of CTMP on PKBα activity in response to physiological stimuli, we treated HEK293 cells transfected with constructs expressing PKBα and various amounts of CTMP with insulin or IGF-1. The kinase activity of PKBα was stimulated by both insulin and IGF-1, and this stimulation was progressively inhibited by increasing amounts of CTMP expression (Fig. 4A). Furthermore, analysis of the phosphorylation status of PKB revealed that CTMP expression led to a decrease in Ser[473] and Thr[308] phosphorylation induced by insulin and IGF-1 (Fig. 4B). These data reinforce the results seen with pervanadate (Fig. 3) and support the hypothesis that CTMP is an inhibitor of PKB in vivo.

To explore the effect of CTMP on downstream effectors of PKB, we analyzed the consequence of CTMP expression on PKBα-mediated transcriptional regulation. PKBα reduces both basal and serum-stimulated transcriptional activity of the c-*fos* promoter (*16*). Coexpression of CTMP completely abolished the inhibitory effect of PKBα on c-*fos*–mediated transcription (Fig. 4C), showing that CTMP inhibitory activity is correlated with a reversion of PKB downstream target function. Indeed, CTMP expression increased c-*fos* promoter activity above control levels, possibly through inhibition of endogenous PKB (Fig. 4C). In addition, expression of CTMP reduced phosphoryl-

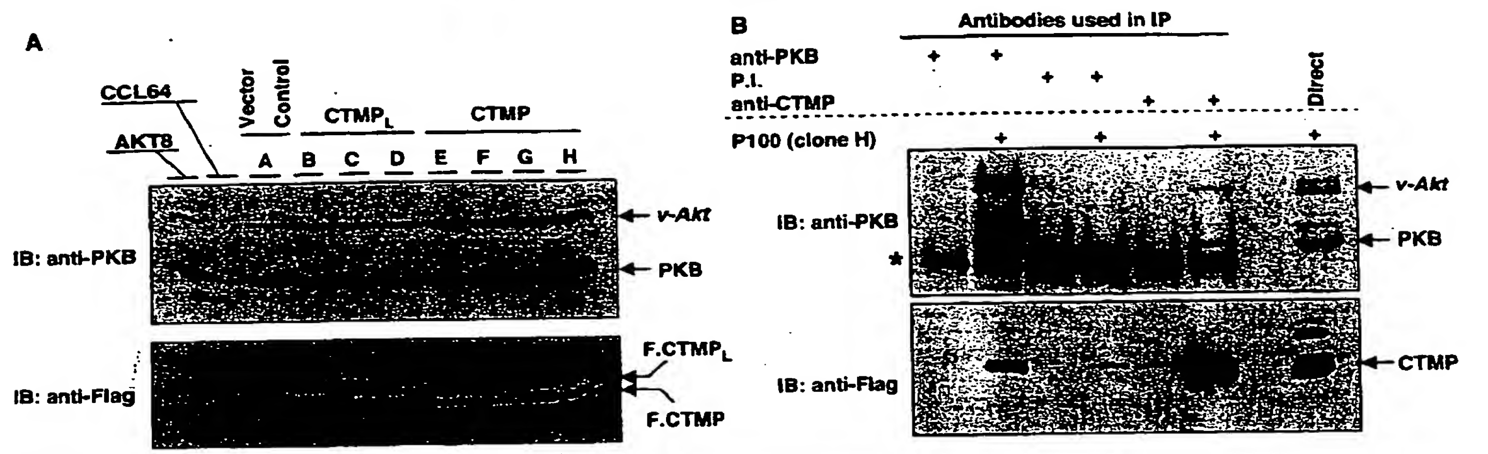

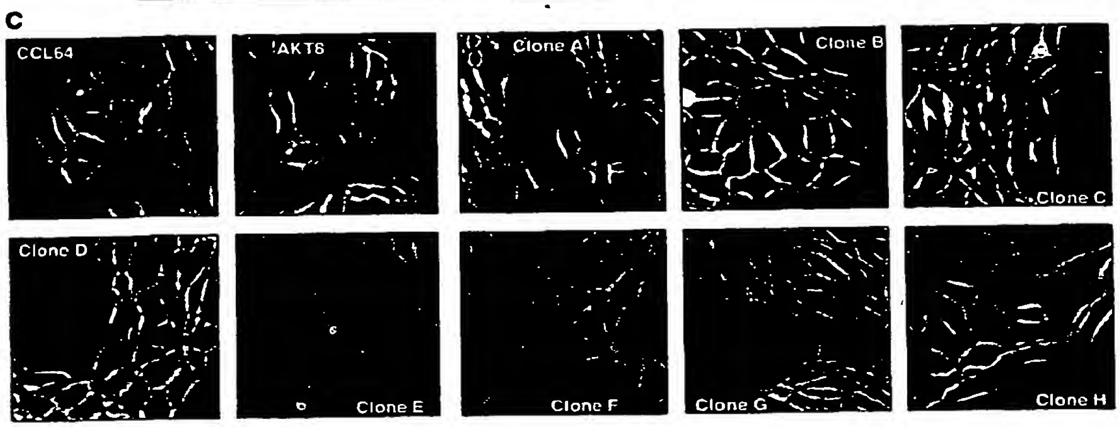

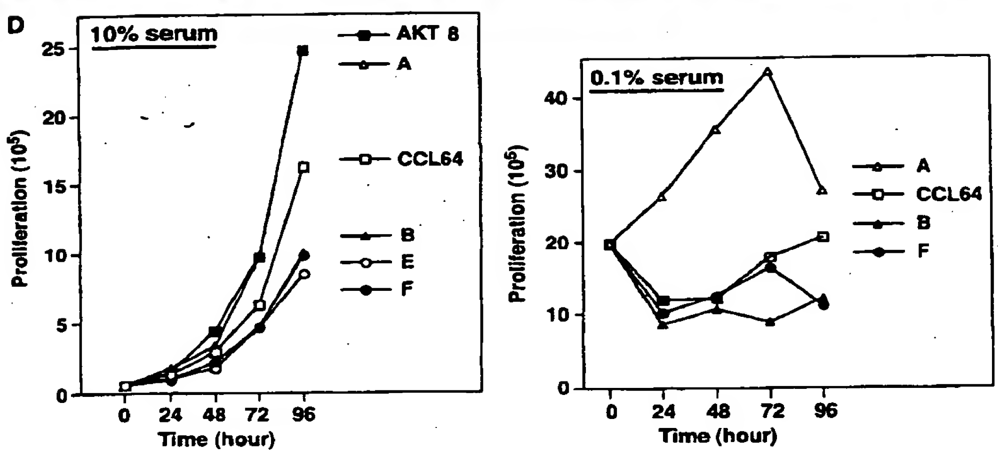

Fig. 5. Phenotypic reversion of v-*Akt*–transformed cells by stable expression of CTMP. **(A)** AKT8 cells were stably transfected with expression vectors for CTMP (pF-CTMP and pF-CTMP$_L$), or with control vector (pSG5-FlagNt-puro). Puromycin-resistant clones were selected and expanded in culture for further characterization (*37*). Selected clones from the empty vector plate (clone A), the pF-CTMP plate (clones E, F, G, and H), or the pF-CTMP$_L$ plate (clones B, C, and D) were analyzed for Akt/PKB (upper panel) and CTMP (bottom panel) expression. **(B)** P100 membrane fraction (500 μg) from clone H prepared in HES buffer (+ lanes) or HES buffer alone were incubated with 10 μg of the indicated antibodies (*14*). Immune complexes were then analyzed by immunoblotting with the indicated antibodies. PKB and CTMP protein migration was confirmed by direct blotting of the P100 fraction (direct). The asterisk shows the IgG heavy chain position. **(C)** CCL64, AKT8, and cells from clones A to H were seeded in a 35-mm dish and photographed with a phase-contrast microscope before reaching confluency. **(D)** Cells from parental cell lines CCL64 and AKT8 [5×10^4 (10% serum, left panel) or 2×10^5 (0.1% serum, right panel)], as well as clones A, B, E, and F were seeded in 35-mm dishes. Cells were trypsinized, and viable cells were counted following staining by trypan blue exclusion at the indicated time for the relevant cell lines.

ation of glycogen synthase kinase–3β (GSK-3β) on Ser[9], a PKB-mediated phosphorylation event (*16*).

To determine the consequence of disrupting CTMP function in vivo, HEK293 cells were transfected with an antisense CTMP expression vector (Fig. 4D). Increasing amounts of antisense CTMP cDNA, confirmed by RT-PCR, increased Ser[473] phosphorylation of endogenous PKB without changing its expression (Fig. 4D). These data demonstrate that inhibition of endogenous CTMP function increases the activation status of endogenous PKBα and indicate that CTMP acts as a negative regulator of PKBα in vivo. Supporting these data, similar increases in endogenous GSK-3β phosphorylation on Ser[9] were also observed in the presence of the antisense CTMP construct, but not a control antisense construct (*16*). This effect is not due to an up-regulation of PI-3 kinase activity, because no increase in the activity of this enzyme was observed when antisense CTMP or a control luciferase antisense cDNA was expressed (*16*). Therefore, ablation of CTMP function increases the ability of PKB to activate its downstream effectors in cells.

CCL64 mink lung cells stably expressing v-*Akt* (AKT8 cells), the viral homolog of PKB isolated from mouse, are transformed and tumorigenic in vitro (*19*–*21*). To expand the hypothesis that CTMP negatively regulates PKBα in vivo and to analyze whether CTMP expression could revert the phenotype of v-*Akt*–transformed cells, AKT8 cells were transfected with the cDNA encoding CTMP (CTMP) or with a cDNA corresponding to the original clone isolated from the two-hybrid analysis (CTMP$_L$). This clone contains an extra 15 amino acids at the NH_2-terminus and was identical to wild-type CTMP in terms of PKBα binding and inhibition (*13*). Clones stably expressing CTMP were selected and analyzed on the basis of three criteria:

100 μM Na_3VO_4, 1 μM microcystin LR, 1 mM phenylmethylsulfonylfluoride (PMSF), and 1 mM benzamidine) by trituration through a 25-gauge needle 25 times. The nuclei were removed by centrifugation, and the P100 and S100 fractions were obtained by centrifugation at 100 000*g* for 30 min at 4°C. P100 fractions were resuspended in HES buffer containing 0.1% NP-40, incubated at 4°C for 60 min, and centrifuged at 10000*g* for 5 min to remove insoluble material. Immunoprecipitations were carried out at 4°C for 2 hours using 5 μg of antibody to Flag (Sigma) for transfected COS-1 cells, or overnight using 5 μg of antibody against PKB, or preimmune or antibodies against CTMP for endogenous complexes in untransfected cells. Immune complexes were precipitated using a 1:1 mixture of protein A–protein G–Sepharose (Amersham Pharmacia). The beads were washed, resuspended in 2X Laemmli buffer, and analyzed by SDS-PAGE and immunoblotting.

32. The PKBα mAb A4D6 was generated by M. Thelen, P. Cron, A. Wetterwald, and B. A. Hemmings (unpublished results).
33. HA-PKBα and HA–m/p-PKBα expression vectors were described previously (*17*). pGST-PKB-RD was generated by cloning an Nde I–Eco RI PCR fragment of PKBα into the corresponding sites of the pBC vector (*26*), referred to as pGST in Fig. 2.
34. Cells were starved for 15 hours in DMEM without serum or phosphate, and then incubated for 4 hours in this medium containing 1 mCi of [^{32}P]orthophosphate. Cells were then lysed, and Flag-CTMP immunoprecipitated as described (*14*).
35. Cells were maintained in DMEM supplemented with 10 % fetal calf serum (FBS, Life Technologies) and 50 U/ml Pen/Strep (Gibco) for COS-1, HeLa, HEK293, CCL64, AKT8 cells, or 10 % calf serum for NIH 3T3 cells. Transfections were performed by using the calcium phosphate technique (*27*). Transfected COS-1 cells or HEK293 cells were scraped in NP-40 lysis buffer (*28*), and lysates were cleared by centrifugation at 10 000*g* for 10 min. HA-PKBα was precipitated with the HA mAb 12CA5 absorbed to protein A–Sepharose (Amersham Pharmacia). Immune complexes were washed once with lysis buffer containing 500 mM NaCl, once with lysis buffer, and once with 50 mM Tris-HCl (pH 7.8), 1 mM PMSF, 1 mM benzamidine. In vitro kinase assays were as described (*28*). When required, cells were stimulated with 0.1 mM pervanadate prepared with 0.2 mM H_2O_2 (*17*).
36. RNA was prepared using the Trizol protocol (Gibco) and reverse transcription reactions were performed using the GeneAmp RNA PCR kit (PE Biosystems). The oligonucleotides T7' and 5'-CTCATCAACACTCT-GAACATT-3' were used in RT-PCR reactions to distinguish the antisense construct from the endogenous CTMP cDNA.
37. Four 10-cm dishes of *AKT8*-transformed CCL64 cells were transfected with 15 μg pSG5 (negative control), or pSG5-FlagNt-puro (empty vector), pF-CTMP or pF-$CTMP_L$ constructs. After transfection, cells were trypsinized and reseeded in three 10-cm dishes in medium containing 2 μg/ml puromycin. Colonies were picked after 7 days and grown to confluency in puromycin-containing medium.
38. We thank P. Cron for dedicated technical assistance; J. F. Spetz and P. Kopp for assistance with the nude mice experiments; A. Matus and J. Hagmann for help with confocal microscopy; B. Chatton (IGBMC, Strasbourg, France) for the pBC vector; J. Hartley (NCI, NIH,) for the CCL64 and AKT8 cell lines; S. Ruscetti (NCI, NIH) for the antibody against Gag; A. Merlo (Kantonspital, Basel) for the LN229, U343MG, and U87MG glioblastoma cell lines; Y. Nagamine for the p-*fos*-Luc reporter gene and M. Hill for advice on cell fractionation experiments. S.-M. M. is the recipient of the EMBO long-term post-doctoral fellowship, and part of this work was supported by the Schweizerische Krebsliga (B.A.H.). The Friedrich Miescher Institute is part of the Novartis Research Foundation.

27 April 2001; accepted 22 August 2001

REPORTS

A Small-Molecule Modulator of Poly-α2,8-Sialic Acid Expression on Cultured Neurons and Tumor Cells

Lara K. Mahal,[1] Neil W. Charter,[2] Kiyohiko Angata,[4] Minoru Fukuda,[4] Daniel E. Koshland Jr.,[2] Carolyn R. Bertozzi[1,2,3*]

Poly-α2,8-sialic acid (PSA) has been implicated in numerous normal and pathological processes, including development, neuronal plasticity, and tumor metastasis. We report that cell surface PSA expression can be reversibly inhibited by a small molecule, *N*-butanoylmannosamine (ManBut). Inhibition occurs through a metabolic mechanism in which ManBut is converted to unnatural sialic acid derivatives that effectively act as chain terminators during cellular PSA biosynthesis. *N*-Propanoylmannosamine (ManProp), which differs from ManBut by a single methylene group, did not inhibit PSA biosynthesis. Modulation of PSA expression by chemical means has a role complementary to genetic and biochemical approaches in the study of complex PSA-mediated events.

The biological functions of cell surface oligosaccharides have been difficult to elucidate owing to the complexity of achieving genetic control over a molecule that is the product of multiple enzymes and thus of multiple genes. In a few well-studied cases, the function of a specific oligosaccharide epitope has been determined, enhancing our understanding of cell-cell recognition (*1*). Still, few such structures have been assigned a specific purpose. Small molecules that disrupt or activate a target process in a cellular context have provided insights in systems that are difficult to manipulate with traditional genetic methods (*2*). The ability to block the expression of a specific oligosaccharide epitope by use of a small molecule would facilitate the study of oligosaccharide function.

PSA (Fig. 1A), a linear homopolymer of α2,8-linked sialic acid residues, is found mainly on the neural cell adhesion molecule (NCAM) (*3*, *4*). Its biosynthesis is mediated by polysialyltransferases, the best-characterized human homologs of which are ST8SiaII (STX) and ST8SiaIV (PST) (*5*–*7*). Both enzymes catalyze the iterative formation of α2,8-sialic acid linkages using cytidine 5'-monophosphate (CMP)–sialic acid as a substrate. PSA is abundant in the central nervous system during fetal development but is restricted to those regions of the adult brain associated with synaptic plasticity (*8*–*10*). In addition, PSA is a marker of several tumors including neuroblastomas, small cell lung carcinomas, and Wilms tumor (*11*, *12*). It has been implicated in tumor metastasis and the complex neural processes involved in learning and memory (*3*, *13*). We report here a small-molecule modulator of PSA expression.

The cellular machinery for conversion of *N*-acetylmannosamine (ManNAc, Fig. 1B) to CMP–sialic acid tolerates conservatively altered *N*-acyl substituents (*14*). Thus, administration of *N*-propanoylmannosamine (ManProp, Fig. 1B) or *N*-butanoylmannosamine (ManBut) to cultured cells and laboratory animals results in biosynthesis of the corresponding CMP–sialic acid analogs and the appearance of unnatural sialic acid residues on cell surface glycoproteins. In most sialoglycoconjugates, sialic acid residues occupy terminal α2,3- or α2,6-linkages to galactose; replacement of some fraction of these residues with an unnatural variant has no discernible effect on their abundance (*15*–*17*). By contrast, in PSA sialic acid occupies both terminal and internal positions, prompting us to consider the effects of incorporation of unnatural sialic acids on its biosynthesis.

We treated NT2 neurons (*18*) with ManProp or ManBut and visualized PSA expression by immunofluorescence microscopy with the monoclonal antibody (mAb) to PSA 12F8 (*19*, *20*). At concentrations up to 10 mM in the culture medium, ManProp had no effect on PSA expression (Fig. 1C). However, ManBut abrogated 12F8 staining in a dose-dependent manner, indicating that it functions as a metabolic inhibitor of PSA expression (*21*).

We also analyzed the effects of ManProp and ManBut on the cellular biosynthesis of PSA associated with NCAM. After incubation with various concentrations of ManProp or ManBut, NT2 cells were lysed and subjected to protein immunoblot analysis with the mAb 735 to PSA and the mAb OB11 to NCAM (*19*). Polysialy-

[1]Department of Chemistry, [2]Department of Molecular and Cell Biology, [3]Howard Hughes Medical Institute, University of California, Berkeley, CA 94720, USA. [4]Glycobiology Program, Cancer Research Center, Burnham Institute, La Jolla, CA 92037, USA.

*To whom correspondence should be addressed. E-mail: bertozzi@cchem.berkeley.edu

THE JOURNAL OF BIOLOGICAL CHEMISTRY
© 1999 by The American Society for Biochemistry and Molecular Biology, Inc.
Vol. 274, No. 40, Issue of October 1, pp. 28803–28807, 1999
Printed in U.S.A.

Isolation of the Protein Kinase TAO2 and Identification of Its Mitogen-activated Protein Kinase/Extracellular Signal-regulated Kinase Kinase Binding Domain*

(Received for publication, June 7, 1999, and in revised form, July 13, 1999)

Zhu Chen‡, Michele Hutchison, and Melanie H. Cobb§
From the Department of Pharmacology, University of Texas Southwestern Medical Center, Dallas, Texas 75235-9041

We previously reported the cloning of the thousand and one-amino acid protein kinase 1 (TAO1), a rat homolog of the *Saccharomyces cerevisiae* protein kinase sterile 20 protein. Here we report the complete sequence and properties of a related rat protein kinase TAO2. Like TAO1, recombinant TAO2 selectively activated mitogen-activated protein/extracellular signal-regulated kinase kinases (MEKs) 3, 4, and 6 of the stress-responsive mitogen-activated protein kinase pathways *in vitro* and copurified with MEK3 endogenous to Sf9 cells. To examine TAO2 interactions with MEKs, the MEK binding domain of TAO2 was localized to an ~135-residue sequence just C-terminal to the TAO2 catalytic domain. *In vitro* this MEK binding domain associated with MEKs 3 and 6 but not MEKs 1, 2, or 4. Using chimeric MEK proteins, we found that the MEK N terminus was sufficient for binding to TAO2. Catalytic activity of full-length TAO2 enhanced its binding to MEKs. However, neither the autophosphorylation of the MEK binding domain of TAO2 nor the activity of MEK itself was required for MEK binding. These results suggest that TAO proteins lie in stress-sensitive kinase cascades and define a mechanism by which these kinases may organize downstream targets.

Ste20p[1] was originally isolated as a gene of budding yeast whose product functioned downstream of the $\beta\gamma$ subunits of a heterotrimeric G protein but upstream of enzymes in the MAP kinase module of the pheromone response pathway (1, 2). Several mammalian protein kinases related to Ste20p have been identified that phosphorylate MAP/ERK kinase (MEK) family members in stress-activated MAP kinase cascades. These include mixed lineage kinases, TGF-β-activated protein kinase, and TAO1 (3–8). In the yeast protein kinase family tree the Ste20p branch is closest to the MEK kinases (MEKKs) (9). Thus, it is not surprising that several mammalian Ste20p-related kinases are MEKKs. Some have selectivity for MEKs in the c-Jun N-terminal kinase/stress-activated protein kinase (JNK/SAPK) pathway and others for the p38 stress-sensitive pathway, whereas most phosphorylate both groups of MEKs *in vitro* (3, 7, 8, 10–13). The plethora of Ste20p-like kinases with effects on stress pathways and their overlapping biochemical activities have made it difficult to define their roles in the physiological regulation of these kinase cascades. MEK3 and MEKK1 are almost certainly important for regulation of JNK/SAPKs because they bind to JNK/SAPK and other cascade components either through a scaffold protein, with a function believed to be analogous to the yeast scaffold protein Ste5p (14, 15), or directly (16, 17). The association of kinases in complexes provides compelling evidence for their interrelated or dependent functions even in the absence of information regarding physiological roles.

To identify novel components of MAP kinase cascades, we isolated several PCR products and cDNAs encoding homologs of Ste20p from *Saccharomyces pombe* and mammals (8, 18, 19). Among the mammalian cDNAs, we isolated one that encoded the protein kinase TAO1, named for its one *t*housand *a*nd *o*ne amino acids. TAO1 is like certain other relatives of Ste20p in that it phosphorylates and activates MEKs from the stress-responsive MAP kinase cascades. Copurification experiments indicated that TAO1 interacted with MEK3, a p38 activator, although direct binding was not demonstrated. These findings suggested that TAO1 forms complexes with components of p38 MAP kinase cascades and may, therefore, be an important regulator of p38-dependent events.

Here we report the isolation of cDNA clones encoding the complete sequence of TAO2, a close relative of TAO1. Both TAO1 and TAO2 are expressed most highly in brain cells, suggesting their tissue-restricted function (8). The *in vitro* substrate specificities of TAO1 and TAO2 are also similar. Importantly, TAO2, like TAO1, copurifies with MEK3 endogenous to Sf9 cells. This suggests that the intracellular specificity of TAO proteins may be determined by their ability to bind stably to a subset of potential MEK substrates. To define the mechanism by which TAO proteins associate with MEKs, we determined that they interacted directly, identified the MEK binding domain of TAO2, and examined the MEK specificity of this domain.

EXPERIMENTAL PROCEDURES

Isolation of cDNA Clones Encoding TAO2—A 420-base pair PCR product was obtained as described (8) using oligonucleotides based on the yeast Ste20p sequence. This product was labeled with [α-^{32}P]dCTP by random priming and used to probe approximately 1.3 × 10^6 plaques

* This work was supported by Grant GM53032 from the National Institutes of Health (to M. H. C.) and by the National Institutes of Health Medical Scientist Training Program and the Perot Family Foundation (to M. H.). The costs of publication of this article were defrayed in part by the payment of page charges. This article must therefore be hereby marked "*advertisement*" in accordance with 18 U.S.C. Section 1734 solely to indicate this fact.
The nucleotide sequence(s) reported in this paper has been submitted to the GenBank™/EBI Data Bank with accession number(s) AF140556.
‡ This work was submitted in partial fulfillment of the requirements for a doctorate of philosophy at the University of Texas Southwestern Medical Center.
§ To whom correspondence should be addressed: Dept. of Pharmacology, University of Texas Southwestern Medical Center, 5323 Harry Hines Blvd., Dallas, TX 75235-9041. Tel.: 214-648-3627; Fax: 214-648-3811; E-mail: mcobb@mednet.swmed.edu.
[1] The abbreviations used are: Ste20p, sterile 20 protein; MAP, mitogen-activated protein; ERK, extracellular signal-regulated protein kinase; MEK, MAP/ERK kinase or MAP kinase kinase; MEKK, MEK kinase; TAO, thousand and one amino acid protein kinase; GST, glutathione *S*-transferase; MBP, myelin basic protein; JNK, c-Jun N-terminal kinase; SAPK, stress-activated protein kinase; PCR, polymerase chain reaction; DTT, dithiothreitol.

a random-primed adult rat forebrain cDNA library and approximately 0.6 × 10^6 plaques of an oligo(dT)-primed rat brain cDNA library (both provided by Jim Boulter, UCLA). cDNA clones encoding TAO1 and TAO2 were obtained. Subsequent rounds of screening yielded the full-length TAO2 cDNA, which was assembled into pBluescript from 3 of over 50 positive clones. The complete sequence of the assembled cDNA was deposited in GenBank™ with the accession number AF140556.

Plasmid Construction—pBluescript-TAO2-(1–320), containing the catalytic domain of TAO2, and a catalytically defective mutant pBluescript-TAO2D169A were generated by PCR. Wild-type TAO2, TAO2D169A, and TAO2-(1–320) were cloned into pRSETB (Invitrogen) to incorporate a $MRGSH_6$ tag and subsequently transferred into the baculoviral shuttle vector pVL1393. Recombinant viruses were selected as described (8). For expression in mammalian cells, the cDNAs encoding these TAO2 proteins were also cloned into pCMV5 that had been modified to place a Myc epitope tag at the N terminus of the encoded protein. A truncated, catalytically defective TAO2 in pRSETB was created by changing lysine 57, in the conserved VAIK motif, to alanine (K57A) by PCR.

For binding assays, fragments of TAO2 were subcloned into pGEX-KG by PCR. TAO2-(314–451) was subsequently transferred into pRSETA utilizing the *Bam*HI and *Eco*RI restriction sites. Catalytically defective MEK3 was created in pNPT7–5 by changing lysine 64 to methionine (K64M). A MEK1/6 chimera, which contains the N-terminal domain of MEK1 and the C-terminal domain of MEK6, and a MEK6/1 chimera with the reciprocal domains (see Fig. 4*B*) were transferred into pRSETA or -C, respectively, from the original pGEX-KG-MEK1/6 and MEK6/1 plasmids (generously provided by Lori Christerson) utilizing the *Bam*HI and *Hin*dIII restriction sites.

Expression and Purification of Recombinant Proteins from Sf9 Cells and Bacteria—Recombinant histidine-tagged TAO2, TAO2-(1–320), and TAO2D169A were expressed and harvested from Sf9 cells as described previously for TAO1 (8). Proteins were adsorbed to Ni^{2+}-nitrilotriacetic acid-agarose (Qiagen) and eluted with a gradient of 20–250 mM imidazole in 0.5 mM dithiothreitol (DTT) and 0.8 M NaCl. His_6-TAO2D169A was further purified on MonoQ (Amersham Pharmacia Biotech) by elution with 50–450 mM NaCl in 1 mM DTT, 0.2 mM EGTA, 1 mM benzamidine, 10% glycerol, and 20 mM Tris, pH 8. TAO2 was detected by Western blotting with an antibody to the $MRGSH_6$ epitope (Qiagen) and silver staining. GST fusion proteins, His_6-tagged TAO2 C-terminal fragments, and other recombinant proteins were expressed and purified from bacteria essentially as described previously (20). Induction of expression was with 30–300 μM isopropyl-1-thio-β-D-galactopyranoside at 25 or 30 °C for 4–16 h, based on individual optimizations.

Immunoprecipitation and Affinity Purification from Transfected 293 Cells and Sf9 Cells—pCMV5-Myc-TAO2 constructs were transfected into 293 cells using calcium phosphate (21). After 48 h, cells were lysed (22), and transfected proteins were detected by anti-Myc Western blotting. Lysate volumes containing equal amounts of expressed protein were used for subsequent immunoprecipitation with anti-Myc antibodies for kinase assays. Sf9 lysates containing His_6-TAO2 proteins were incubated with Ni^{2+}-nitrilotriacetic acid-agarose in buffer containing 0.15 M NaCl and 0.5 mM DTT and washed with 0.3 M NaCl, 0.5 mM DTT, and 10 mM imidazole. Bound proteins were eluted with 250 mM imidazole in buffer and subjected to Western blotting with an anti-MEK3 antibody (23).

In Vitro Kinase Assays—Kinase assays contained 50 mM HEPES, pH 8, 10 mM $MgCl_2$, 1 mM DTT, 0.5 mg/ml myelin basic protein (MBP), and 100 μM ATP ([γ-^{32}P]ATP, 2–7 cpm/fmol). Reactions were halted with 10 μl of 5× electrophoresis sample buffer, followed by boiling, and 20 μl were analyzed by SDS-polyacrylamide gel electrophoresis and autoradiography. For linked kinase assays, 50–250 ng of recombinant TAO2 protein was incubated with 50 ng of MEK proteins in 30 μl for 60 min at 30 °C; 5 μl of the reactions were added to second reactions containing K52R ERK2, p38, or GST-SAPKβ (23, 24) at 10 μg/ml. Phosphoamino acids were determined as described (25).

In Vitro Binding Assays—For binding assays involving GST-tagged TAO2 fragments and His_6-tagged MEK proteins, 3 μg of each GST fusion protein or GST alone was incubated with glutathione-agarose beads at 4 °C in the presence of 0.1 mg/ml bovine serum albumin for 30 min and washed with 0.1 M NaCl in 50 mM Tris, pH 7.4. 5 μg of His_6-tagged protein were incubated with the beads in the presence of 0.1 mg/ml bovine serum albumin and 0.1 M NaCl at 4 °C for 1 h. The beads were washed with 0.3 M NaCl, 0.1% Triton X-100, and 50 mM Tris, pH 7.4. Bound proteins were released with 1× SDS electrophoresis sample buffer and subjected to anti-His_6 Western blotting. Similar binding assays were performed for His_6-TAO2-(314–451) and GST-tagged MEK proteins.

RESULTS

Isolation of TAO2 cDNAs—Degenerate oligonucleotide primers designed from the sequence of the *Saccharomyces cerevisiae* Ste20p kinase were used in PCR to amplify fragments of related protein kinases from rat cDNAs. One PCR product was used in isolating overlapping cDNAs from two rat brain cDNA libraries that encoded two protein kinases, TAO1 (8) and the related kinase TAO2, described here. The assembled TAO2 cDNA predicted an open reading frame of 993 amino acids (Fig. 1*A*). The presumed start codon is located at base 193 and is preceded by an in-frame stop codon at base 145. The longest 3′-untranslated region was 1317 base pairs in length, including a poly(A) track at its end, ~1.3 kilobase pairs 3′ to the stop codon (not shown).

Amino Acid Sequence of TAO2—The deduced TAO2 protein has a calculated molecular mass of 114 kDa. The serine/threonine protein kinase catalytic domain is at its N terminus. In its 690 C-terminal residues, TAO2 contains a possible nucleotide binding site, a serine-rich region, and a proline and leucine-rich region, all shared with TAO1, and an unbroken stretch of 17 glutamic acid residues unique to TAO2. Like TAO1, TAO2 does not appear to contain a small G protein binding consensus motif found in several other Ste20p relatives (14). The TAO2 protein kinase domain displays 90 and 63% identity to TAO1 and the *Caenorhabditis elegans* TAO ortholog (CeTAO, accession number U32275), respectively (not shown). TAO2 displays marked similarities to TAO1 and the *C. elegans* kinase outside the catalytic domain (Fig. 1*B*).

Expression and Activity of TAO2—Truncated, recombinant TAO2-(1–320) purified from Sf9 cells phosphorylated MBP with a specific activity of 0.6 μmol·min^{-1}·mg^{-1}. The full-length protein purified on MonoQ had lower intrinsic activity, about 10% of the truncated enzyme (not shown). Kinase-deficient mutants, His_6-TAO2D169A expressed in Sf9 cells and purified on MonoQ or His_6-TAO2K57A expressed in bacteria, were inactive toward MBP *in vitro*. TAO2 and TAO2-(1–320) expressed in either Sf9 or mammalian cells autophosphorylated extensively on serine and threonine residues (data not shown).

TAO2 Activates MEK3, MEK4, and MEK6 in Vitro—TAO1 was previously shown to activate MEKs 3, 4, and 6 *in vitro*. We therefore examined the ability of TAO2 to activate MEK family members. TAO2-(1–320) produced in Sf9 cells was subjected to a linked kinase assay by incubating it with recombinant MEKs produced in bacteria in the presence of ATP. Aliquots of the first stage reactions were transferred to second reactions to measure the phosphorylation of appropriate MAP kinase substrates by the recombinant MEKs (Fig. 2*A*). TAO2-(1–320) activated MEK3 and MEK6 40- and 20-fold, respectively, toward their substrate p38 (Fig. 2*B*). TAO2 also increased the ability of MEK4 to phosphorylate its substrate SAPK by 7-fold. TAO2-(1–320) was unable to increase the activity of MEK1 or MEK2 toward their substrate K52R ERK2. Full-length TAO2 displayed about 20% of the MEK3-activating ability of TAO2-(1–320), consistent with its lower activity toward MBP. Neither TAO2 mutants D169A nor K57A activated any of the MEKs (data not shown). TAO2-(1–320) expressed in 293 cells also enhanced the ability of MEK3 and MEK4 to phosphorylate their substrates (not shown).

TAO2 Interacts with MEK3—We found that recombinant TAO1 copurified with MEK3 endogenous to Sf9 cells, and overexpressed TAO1 interacted with MEK3 in 293 cells (8). These observations led us to investigate whether TAO2 has similar properties. TAO2 proteins overexpressed in Sf9 cells (Fig. 3*A*) were purified on nickel resin and immunoblotted for MEK3. As

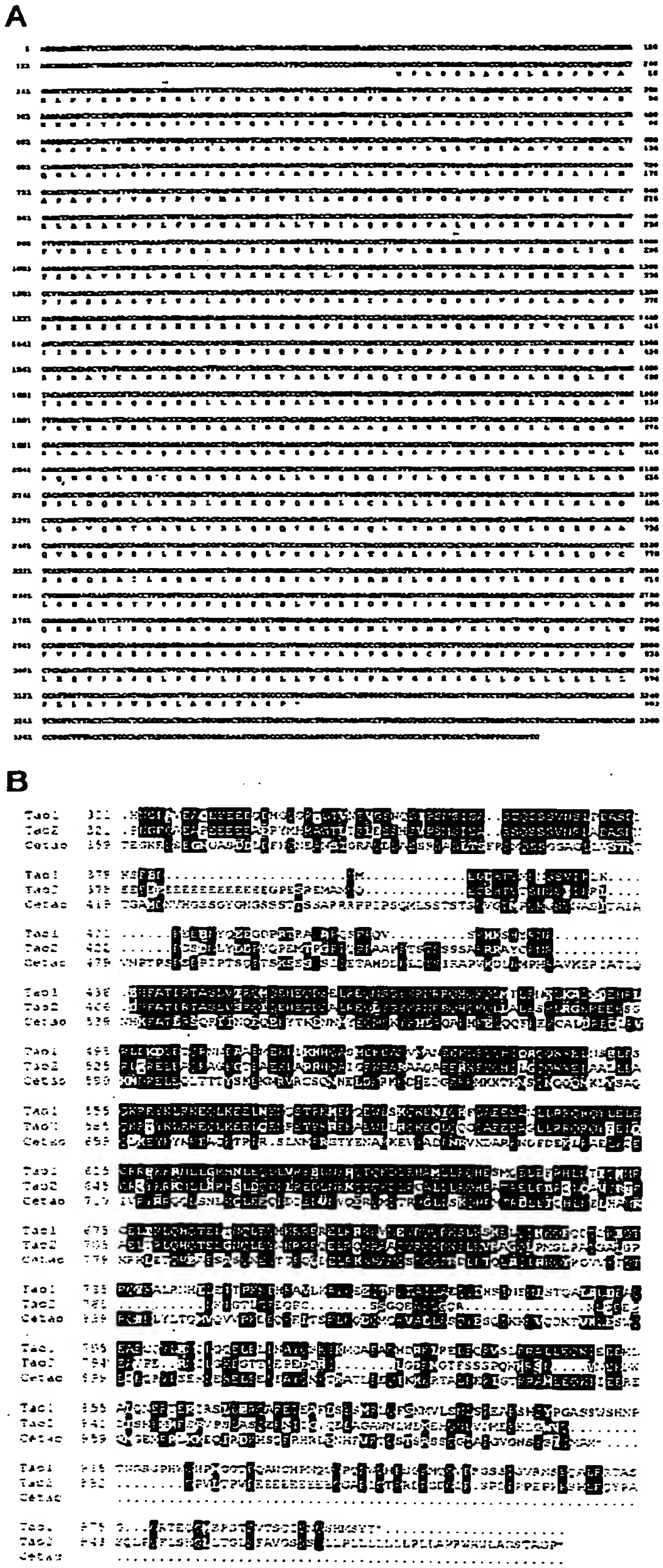

FIG. 1. **Nucleotide and protein sequence of TAO2.** *A*, the complete amino acid sequence of TAO2 is indicated *below* the nucleotide sequence. Most of the 3′-untranslated region is not shown but was deposited in GenBank™ (accession number AF140556). The boundaries of the minimal catalytic domain are denoted by the *arrows above* residues 25 and 285. *B*, the alignment of the noncatalytic domains of TAO1 and CeTAO, the *C. elegans* TAO ortholog (8), with TAO2 residues 321–993 demonstrates significant similarity outside their kinase domains. Identical residues are *boxed* in *black* and conserved residues are *shaded*.

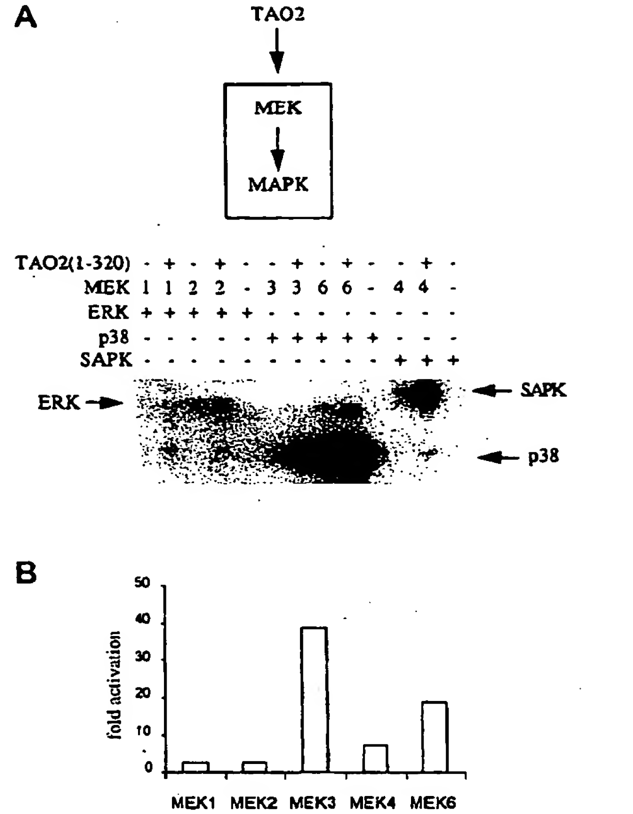

FIG. 2. **TAO2 has MEKK activity.** *A*, linked kinase assays were used to measure activation of various MEK family members by recombinant TAO2-(1–320) purified from Sf9 cells. Phosphorylation of appropriate MAP kinase substrates by the MEK family members in second reactions are shown. *B*, data represented in *A* have been quantitated and are plotted as -fold activation of MEKs by TAO2-(1–320). One of five similar experiments is shown.

a control, Sf9 cell lysates not expressing TAO2 were processed similarly. MEK3 endogenous to Sf9 cells was associated with full-length, wild-type TAO2 (Fig. 3*B*, *lane 2*; Fig. 3*C*, *lane 1*) but not TAO2D169A (Fig. 3*C*, *lane 2*), TAO2-(1–320) (Fig. 3*B*, *lane 3*), or beads incubated with lysates from uninfected Sf9 cells (Fig. 3*B*, *lane 1*; Fig. 3*C*, *lane 3*). These results demonstrated that TAO2 binds to MEK3, the interaction is mediated by the noncatalytic region of the protein, and TAO2 catalytic activity enhances MEK3 binding to the full-length protein.

To determine the domain in TAO2 that mediates the interaction with MEK3, the series of fragments that span the noncatalytic domains of TAO2 were expressed as GST fusion proteins and tested for their abilities to bind His_6-MEK3 *in vitro* (Fig. 3*D*). The MEK3 binding domain was localized to an ~135-residue region, residues 314–451, just C-terminal to the TAO2 catalytic domain. This region was further subdivided, but all of the shorter fragments containing residues 395–451 were degraded. TAO2-(314–377), which precedes the polyglutamic acid region, was insufficient for MEK3 binding.

TAO2 Binds MEKs 3 and 6 in Vitro but Not MEKs 1, 2, or 4—To investigate the binding specificity of the TAO2 MEK binding domain, His_6-tagged MEK proteins were compared for their capacity to bind to TAO2-(314–451). The TAO2 fragment bound MEK6 in addition to MEK3 but not MEK1, MEK2, or MEK4 (Fig. 4, *A* and *D*). Binding to both MEK3 and MEK6 is

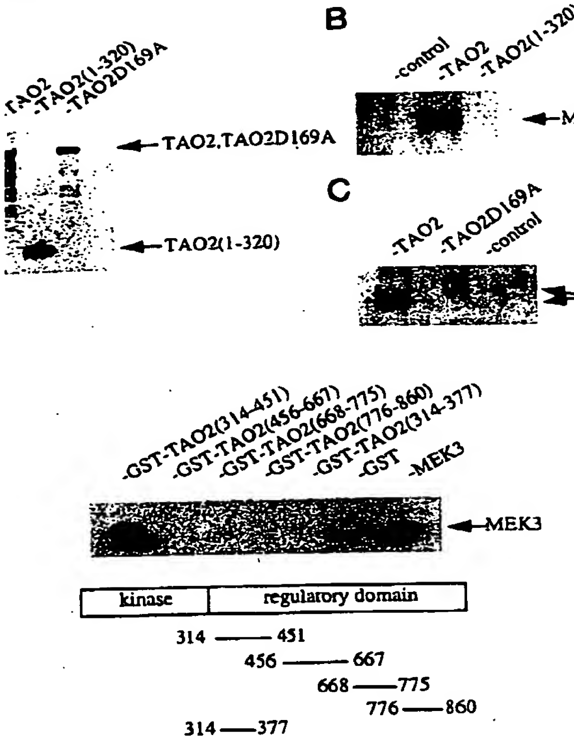

ɪG. 3. **Identification of the TAO2 MEK binding domain.** *A*, $_6$-tagged TAO2, TAO2-(1–320), and TAO2D169A were expressed in arate batches of Sf9 cells, and the proteins were detected with an ibody that recognizes the N-terminal epitope. Comparable amounts 'AO2 proteins were detected in each lysate. *B* and *C*, His$_6$-tagged)2, TAO2-(1–320), and TAO2D169A were purified from cell lysates Ni^{2+}-nitrilotriacetic acid-agarose and subjected to anti-MEK3 West- blotting to detect associated MEK3 that was endogenous to Sf9 s. Lysates from Sf9 cells not expressing recombinant protein were cessed as a control. One of three comparable experiments is shown. : same experiment was also performed in Sf900 cells with a similar ult. *D*, TAO2 C-terminal fragments were expressed as GST fusion teins in bacteria and tested for MEK3 binding activity. MEK3 bind- was measured by immunoblotting the proteins bound to the beads h anti-His$_6$ antibodies. His$_6$-MEK3 was loaded in the *last lane* as itive control. Binding reactions were performed from five to eight ɪes for the various TAO2 fragments.

ısistent with their significant sequence similarity compared :h the other MEK family members. Chimeric proteins gen- ıted from MEK6 and MEK1 (Fig. 4*B*) were used to determine : portion of the MEK that binds to the TAO2 domain. His$_6$-:K1/6 was unable to bind to TAO2-(314–451), whereas GST-:K6/1 is as efficient as GST-MEK6 in binding to the TAO2 ·gment (Fig. 4, *C* and *D*).

As noted earlier, catalytically defective TAO2 was deficient MEK3 binding. To explore the underlying reason, we asked ıether autophosphorylation of TAO2 might have an effect on ability to bind to MEK3. The MEK3 binding fragment of .O2 was autophosphorylated by the catalytic domain of .O2 on both serine and threonine residues (Fig. 5, *A* and *B*). :, thus, first phosphorylated TAO2-(314–451) with TAO-(1– 0) for different lengths of time to determine whether phos- orylation would alter its binding activity. Different concen- ıtions of ATP and Mg^{2+} were also tested in the binding assay. :tle or no effect of the autophosphorylation state or ΓP·Mg^{2+}] on MEK3 binding activity was observed (Fig. 5*C*). determine whether MEK3 kinase activity was necessary for ıding to TAO2, the binding of kinase-inactive MEK3 (K64M) ıs tested (Fig. 5*D*). This defective mutant binds to TAO2 as ıll as wild-type MEK3, suggesting that MEK3 kinase activity dispensable for interaction with TAO2.

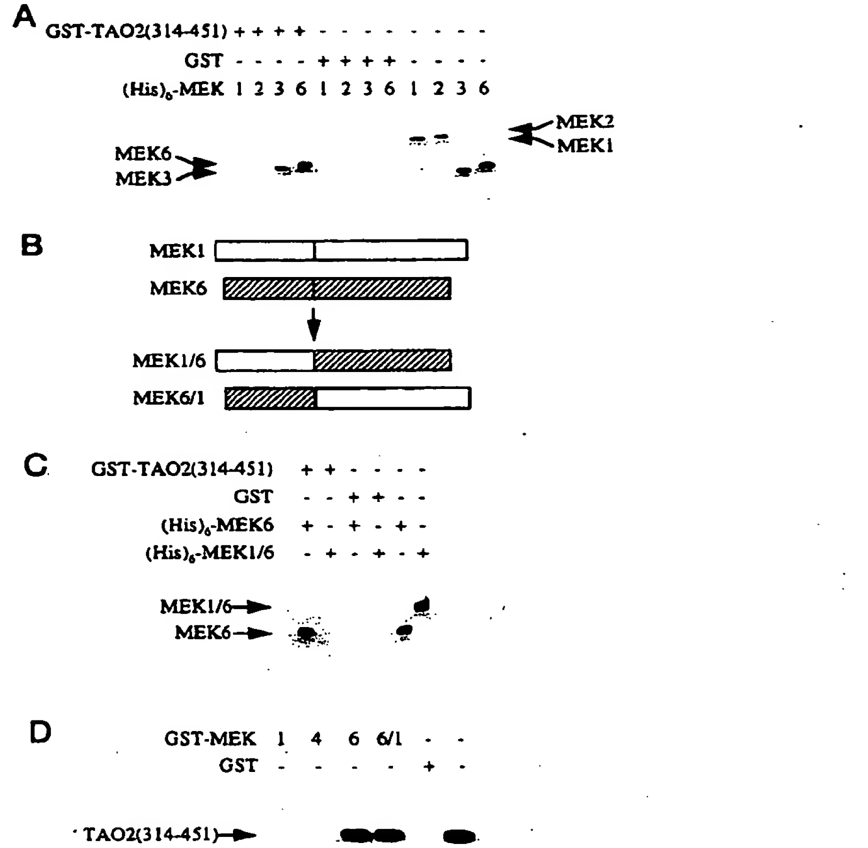

FIG. 4. **Specificity of MEK binding to TAO2-(314–451).** *A*, binding of GST-TAO2-(314–451) to His$_6$-tagged MEK family members. The MEK family members associated with bead-bound GST-TAO2-(314–451) were detected using anti-His$_6$ antibodies. The *last four lanes* contain purified MEK1, -2, -3, and -6, respectively, to show their positions on the gel. One of three similar experiments is shown. *B*, chimeric proteins were derived from MEK6 and MEK1. MEK1/6 consists of the N terminus of MEK1 and the C terminus of MEK6, whereas the reciprocal chimera MEK6/1 consists of the N terminus of MEK6 and the C terminus of MEK1. *C*, binding of GST-TAO2-(314–451) to His$_6$-tagged MEK6 or MEK1/6. MEK1/6 chimeras were used to determine the portion of MEK6 involved in TAO2 binding as described in the legend to *A*. One of two similar experiments is shown. *D*, binding of His$_6$-TAO2-(314–451) to GST-tagged MEK1, -4, -6, or -6/1. Binding to MEK4 was tested, and the tags on the MEK family members and TAO2 proteins were reversed to confirm that the tags had no effect on their protein-protein association. Binding was detected as in *A*. His$_6$-TAO2-(314–451) was loaded in the *last lane* as a positive control. One of two similar experiments is shown.

DISCUSSION

We isolated cDNAs encoding TAO2, a homolog of the previously reported TAO1 (8). We found that TAO2, like TAO1, activated MEKs in the stress-responsive MAP kinase pathways and displayed stable binding to MEK3 endogenous to Sf9 cells. In examining TAO2 expressed in Sf9 cells, we found that the full-length enzyme was significantly less active than the truncated kinase. Thus, the full-length protein was inhibited relative to its truncated forms. Subsequent work indicated that full-length TAO1 is also less active than proteins with C-terminal domain truncations. The inherently higher activity of fragments of TAO1 and -2 suggested that we may have removed an autoinhibitory or pseudosubstrate domain. However, we have not yet identified such a domain, as none of the recombinant fragments from the putative regulatory domain of TAO2 inhibited the activity of its catalytic domain (not shown).

Because TAO2 was purified in a stable complex with MEK3

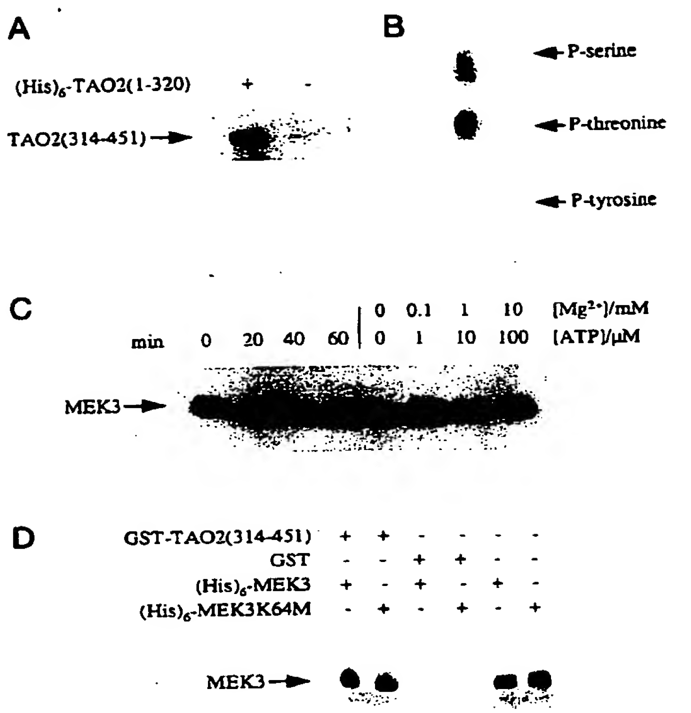

Fig. 5. Neither MEK activity nor autophosphorylation of its MEK binding domain by TAO2 is required for MEK binding to TAO2. *A*, 5 μg of TAO2-(314–451) was incubated with or without 1 μg of His$_6$-TAO2-(1–320) under phosphorylating conditions. The reaction mixture was resolved by SDS-polyacrylamide gel electrophoresis and subjected to autoradiography to detect phosphorylation of the MEK binding site in TAO2. One of three similar experiments is shown. *B*, the labeled TAO2-(314–451) band in *A* was excised and subjected to phosphoamino acid analysis. Migration of phosphoamino acids was determined by ninhydrin staining of unlabeled standards. *C*, GST-TAO2-(314–451) was incubated with His$_6$-TAO2-(1–320) in the presence of Ni^{2+}-nitrilotriacetic acid-agarose under phosphorylating conditions for different lengths of time. Reactions were stopped by transferring to 4 °C and sedimenting the beads to remove the active TAO2 fragment. Supernatants were subjected to binding assays with His$_6$-MEK3 (*left*) as described in the legend to Fig. 4*A*. The indicated concentrations of ATP and Mg^{2+} were tested for their effects on binding (*right*). One of two simlar experiments is shown. *D*, binding of GST-TAO2-(314–451) to His$_6$-tagged MEK3 or kinase-defective MEK3 (K64M). Binding was detected as described in the legend to Fig. 4*A*. One of three similar experiments is shown.

endogenous to Sf9 cells, we localized the MEK binding domain to a small, ~135-amino acid fragment, residues 314–451, just C-terminal to the catalytic domain of TAO2. The N-terminal half of this fragment, residues 314–377, did not bind to MEK3. Because TAO1 and TAO2 both bind MEKs but TAO1 has no polyglutamate stretch, it seems unlikely that these residues participate in MEK binding. Thus, residues from 395 to 451 are most likely required for the stable association with MEKs. These results are consistent with the weak binding of TAO1-(1–416) to MEK3 compared with the strong binding displayed by full-length TAO1 (8) and suggest that residues 404–446, which are well conserved between TAO2 and TAO1, contain the MEK binding domain.

Because TAO1 and -2 can activate MEKs 3, 4, and 6 *in vitro*, we determined the specificity of the MEK binding domain of TAO2. We found that TAO2 binds to MEK3 and MEK6, but not to MEK4, despite the fact that MEK4 is an *in vitro* substrate. The N terminus of the MEK is required for this binding, whereas the C terminus is dispensable. This behavior may be a general property of the organization of MAP kinase cascades. The N termini of other MEK family members contain binding domains for proteins in their cascades. MEK1 binds with high affinity to ERK2 through a basic motif N-terminal to its catalytic domain. MEK1 has been proposed to retain ERK2 in the cytoplasm of unstimulated cells through binding to this site (26), and activation of ERK2 may be impaired if this binding domain is absent.[2] MEK4 is reported to require its N-terminal extension to interact with both MEKK1, an activator, and its substrates, JNK/SAPKs (17). An inhibitory interaction between MEK4 and JNK/SAPKs has also been mapped to this N-terminal domain.[3] This suggests that the stable association of MEK3 or MEK6 with TAO proteins will link their physiological functions to p38 but not JNK/SAPK pathways by restricting their intracellular targets. Future biochemical studies will focus on determining the functions of the other domains of TAO1 and TAO2.

Acknowledgments—We thank Lori Christerson and Alf Dang (UT Southwestern) for critical reading of the manuscript, Lori Christerson and Colleen Vanderbilt for providing MEK1/6 and 6/1 chimeras, Signal Pharmaceuticals for the MEK6 cDNA, Alf Dang for help with data analysis, and Peiqun Wu and Don Arnette for MEK proteins. We particularly thank Jim Boulter (UCLA) for providing several rat cDNA libraries.

REFERENCES

1. Ramer, S. W., and Davis, R. W. (1993) *Proc. Natl. Acad. Sci. U. S. A.* **90**, 452–456
2. Leberer, E., Dignard, D., Harcus, D., Thomas, D. Y., and Whiteway, M. (1992) *EMBO J.* **11**, 4815–4824
3. Hirai, S., Katoh, M., Terada, M., Kyriakis, J. M., Zon, L. I., Rana, A., Avruch, J., and Ohno, S. (1997) *J. Biol. Chem.* **272**, 15167–15173
4. Dorow, D. S., Devereux, L., Tu, G. F., Price, G., Nicholl, J. K., Sutherland, G. R., and Simpson, R. J. (1995) *Eur. J. Biochem.* **234**, 492–500
5. Katoh, M., Hirai, M., Sugimura, T., and Terada, M. (1995) *Oncogene* **10**, 1447–1451
6. Tibbles, L. A., Ing, Y. L., Kiefer, F., Chan, J., Iscove, N., Woodgett, J. R., and Lassam, N. J. (1996) *EMBO J.* **15**, 7026–7035
7. Rana, A., Gallo, K., Godowski, P., Hirai, S., Ohno, S., Zon, L. I., Kyriakis, J. M., and Avruch, J. (1996) *J. Biol. Chem.* **271**, 19025–19028
8. Hutchison, M., Berman, K. S., and Cobb, M. H. (1998) *J. Biol. Chem.* **273**, 28625–28632
9. Hunter, T., and Plowman, G. D. (1997) *Trends Biochem. Sci.* **22**, 18–22
10. Fan, G., Merritt, S. E., Kortenjann, M., Shaw, P. E., and Holzman, L. R. (1996) *J. Biol. Chem.* **271**, 24788–24793
11. Shirakabe, K., Yamaguchi, K., Shibuya, H., Irie, K., Matsuda, S., Moriguchi, T., Gotoh, Y., Matsumoto, K., and Nishida, E. (1997) *J. Biol. Chem.* **272**, 8141–8144
12. Ichijo, H., Nishida, E., Irie, K., ten Dijke, P., Saitoh, M., Moriguchi, T., Takagi, M., Matsumoto, K., Miyazono, K., and Gotoh, Y. (1997) *Science* **275**, 90–94
13. Hirai, S., Noda, K., Moriguchi, T., Nishida, E., Yamashita, A., Deyama, T., Fukuyama, K., and Ohno, S. (1998) *J. Biol. Chem.* **273**, 7406–7412
14. Burbelo, P. D., Drechsel, D., and Hall, A. (1995) *J. Biol. Chem.* **270**, 29071–29074
15. Whitmarsh, A. J., Cavanagh, J., Tournier, C., Yasuda, J., and Davis, R. J. (1998) *Science* **281**, 1671–1674
16. Xu, S., and Cobb, M. H. (1997) *J. Biol. Chem.* **272**, 32056–32060
17. Xia, Y., Wu, Z., Su, B., Murray, B., and Karin, M. (1998) *Genes Dev.* **12**, 3369–3381
18. Marcus, S., Polverino, A., Chang, E., Robbins, D., Cobb, M. H., and Wigler, M. H. (1995) *Proc. Natl. Acad. Sci. U. S. A.* **92**, 6180–6184
19. Polverino, A., Frost, J., Yang, P., Hutchison, M., Neiman, A. M., Cobb, M. H., and Marcus, S. (1995) *J. Biol. Chem.* **270**, 26067–26070
20. Guan, K. L., and Dixon, J. E. (1991) *Anal. Biochem.* **192**, 262–267
21. Sambrook, J., Fritsch, E. F., and Maniatis, T. (1989) *Molecular Cloning: A Laboratory Manual*, Cold Spring Harbor Laboratory, Cold Spring Harbor, NY
22. Frost, J., Xu, S., Hutchison, M., Marcus, S., and Cobb, M. H. (1996) *Mol. Cell. Biol.* **16**, 3707–3713
23. Khokhlatchev, A., Xu, S., English, J., Wu, P., Schaefer, E., and Cobb, M. H. (1997) *J. Biol. Chem.* **272**, 11057–11062
24. Robinson, M. J., Cheng, M., Khokhlatchev, A., Ebert, D., Ahn, N., Guan, K.-L., Stein, B., Goldsmith, E., and Cobb, M. H. (1996) *J. Biol. Chem.* **271**, 29734–29739
25. Boyle, W. J., van der Geer, P., and Hunter, T. (1991) *Methods Enzymol.* **201**, 110–149
26. Fukuda, M., Gotoh, Y., and Nishida, E. (1997) *EMBO J.* **16**, 1901–1908

[2] B. Xu, J. Wilsbacher, T. Collisson, and M. Cobb, manuscript in preparation.
[3] B. J. Mayer, personal communication.

BIOCHIMICA ET BIOPHYSICA ACTA
BBA

ELSEVIER

Biochimica et Biophysica Acta 1381 (1998) 49–60

Characterization of pI_{Cln} phosphorylation state and a pI_{Cln}-associated protein kinase

Roberto Sanchez-Olea [a], Francesco Emma [b], Matthew Coghlan [c], Kevin Strange [a,*]

[a] *Critical Care Research Laboratories, Department of Anesthesia, Harvard Medical School, Boston, MA 02115, USA*
[b] *Department of Medicine, Division of Nephrology, Children's Hospital, Harvard Medical School, Boston, MA 02115, USA*
[c] *Division of Signal Transduction, Beth Israel Hospital, Harvard Medical School, Boston, MA 02115, USA*

Received 16 October 1997; revised 5 January 1998; accepted 13 January 1998

Abstract

pI_{Cln} is a ubiquitous cellular protein that has been proposed to be a volume-sensitive Cl^- channel or a channel regulator. Detailed biochemical, cellular and molecular characterization of pI_{Cln} is required to understand its function. Our goal in the present investigation was to define further the biochemical properties of pI_{Cln} and the proteins that associate with it. Immunoprecipitation of pI_{Cln} from ^{32}P-orthophosphoric acid-labeled C6 glioma cells revealed that the protein is phosphorylated constitutively, primarily on serine residues. Protein kinase activity was detected in pI_{Cln} immunoprecipitates, revealing that a constitutively active protein kinase co-precipitates with pI_{Cln}. A specific association between pI_{Cln} and a protein kinase was also observed in affinity assays using a recombinant GST-pI_{Cln} fusion protein. The pI_{Cln}-associated kinase displayed broad substrate specificity and was inhibited in a concentration-dependent manner by heparin, zinc and 5,6-dichloro-1-β-D-ribofuranosylbenose (DRB). These characteristics resembled those of casein kinase I and II. The pI_{Cln}-associated kinase was not recognized, however, by antibodies against these two enzymes. Association of the kinase with pI_{Cln} was disrupted by increasing concentrations of NaCl in the washing buffer, suggesting that electrostatic interactions are involved in kinase binding. Mutagenesis experiments corroborated this observation. Truncation of pI_{Cln} demonstrated that two highly charged clusters of acidic amino acid residues are both necessary and sufficient for kinase binding. Phosphopeptide mapping demonstrated that pI_{Cln} contains at least two phosphorylated serine residues that are located on trypsin cleavage fragments rich in acidic amino acid residues. We propose that the kinase or a kinase binding protein binds to acidic amino acids located between D101 and Y156 and phosphorylates nearby serine residues.

Keywords: Anion channel; Cell volume regulation; Cell swelling

1. Introduction

I_{Cln} is a Cl^- current induced by overexpression of I_{Cln} cRNA in *Xenopus* oocytes [1]. The cDNA re-

* Corresponding author. Laboratory of Cellular and Molecular Physiology, Department of Anesthesiology, Vanderbilt University Medical Center, 504 Oxford House, 1313 21st Avenue South, Nashville, TN 37232, USA. Fax: +1-615-343-3916; E-mail: kevin.strange@mcmail.vanderbilt.edu

0304-4165/98/$19.00
PII S0304-4165(98)00009-9

sponsible for inducing I_{Cln} was cloned originally from MDCK cells, but the gene is found ubiquitously in mammalian cells [1–4], and is also present in evolutionarily more ancient vertebrates such as *Xenopus laevis* [2] and zebra fish [5]. When expressed in oocytes, the channel responsible for I_{Cln} is constitutively active, has broad anion selectivity, is outwardly rectifying, is inactivated by strong depolarization, and is blocked by extracellular nucleotides such as cAMP and ATP [1]. These characteristics resemble those of an ubiquitous, swelling-activated, outwardly rectifying anion current, $I_{Cl, swell}$. We have termed the channel responsible for $I_{Cl, swell}$ VSOAC (Volume-Sensitive organic Osmolyte/Anion Channel). VSOAC appears to mediate swelling-induced efflux of both Cl^- and uncharged organic osmolytes [6,7]. The channel giving rise to I_{Cln} has been proposed to be the channel responsible for $I_{Cl, swell}$ (i.e., VSOAC) [2,8,9]. More recently, however, it has been suggested that VSOAC and the I_{Cln} channel are distinct molecular species [10,11].

The I_{Cln} protein, pI_{Cln}, is an abundant and ubiquitous cellular protein (e.g., [1–4]). In their original study, Paulmichl et al. [1] argued that pI_{Cln} forms a Cl^- channel with a β barrel pore structure. Subsequently, however, Krapivinsky et al. [2] concluded that pI_{Cln} is not a channel, but is instead a channel regulator. Their conclusion was based on the observation that pI_{Cln} is an acidic, water soluble protein located primarily in the cell cytoplasm. Krapivinsky et al. [2] suggested that overexpression of pI_{Cln} in oocytes activated an endogenous VSOAC [2,12,13].

An understanding of the role, if any, of pI_{Cln} in VSOAC activity and volume homeostasis requires extensive biochemical, cellular and molecular characterization of the protein. Our goal in the present investigation was to define further the biochemical properties of pI_{Cln} and the proteins that associate with it. pI_{Cln} contains consensus sites for phosphorylation by a number of different kinases (see Section 4 and Fig. 7). This suggested that pI_{Cln} is a phosphoprotein and that phosphorylation may control its functional properties. We demonstrate here that pI_{Cln} is phosphorylated in vivo, that it associates selectively in vitro with a constitutively active serine–threonine kinase, and that clusters of acidic amino acids on the protein are important for kinase binding.

2. Experimental

2.1. Cell culture

Rat C6 glioma cells were cultured to near confluency in Eagle's minimal essential medium (MEM; Gibco, Gaithersburg, MD) with 10% fetal bovine serum (FBS; HYCLONE, Logan, UT) and penicillin/streptomycin as described previously [14].

2.2. Antibody production

A fusion protein consisting of full length pI_{Cln} cloned from rat C6 glioma cells fused to glutathione S-transferase (GST) was generated in BL21 *E. coli* using a commercially available kit (Pharmacia Biotech, Piscataway, NJ). The GST-pI_{Cln} fusion protein was purified using Glutathione Sepharose 4B, pI_{Cln} was cleaved from GST with thrombin, and the protein was injected intradermally and intramuscularly into rabbits to generate polyclonal antibodies. Preimmune and immune sera were harvested and stored frozen at −20°C.

2.3. Immunoprecipitation

C6 cells were grown to near confluency in 100 mm diameter tissue culture plates, washed briefly with phosphate-buffered saline (PBS; 2.7 mM KCl, 144 mM NaCl, 1.5 mM KH_2PO_4, 8.1 mM Na_2HPO_4, pH 7.4) and scraped into 0.5 ml of ice-cold lysis buffer (20 mM KCl, 50 mM tris, pH 7.4, 3 mM $MgCl_2$, 1 mM EGTA, 1 mM DTT, 0.5% NP-40, 1 mM Na_3VO_4, 20 mM NaF, pH 7.4) containing protease inhibitors (10 μg/ml leupeptin, 10 μg/ml pepstatin, 10 μg/ml aprotinin, and 1 mM phenylmethanesulfonyl fluoride [PMSF]). After incubating for 20 min on ice, the cell lysate was centrifuged at 14,000 rpm for 10 min. pI_{Cln} and associated proteins were immunoprecipitated by adding 10 μl of anti-pI_{Cln} polyclonal antiserum to each 0.5 ml of supernatant and incubating for 2 h at 4°C. Protein A-agarose (Santa Cruz Biotechnology, Santa Cruz, CA) was added as a slurry of 20 μl for every 0.5 ml of supernatant and incubated for 2 h at 4°C on a Labquake Shaker (Labindustries, Berkeley, CA). The resin was then washed five times with ice-cold lysis buffer without protease inhibitors. Proteins were dis-

ociated from the resin by boiling for 4 min and then esolved by SDS-PAGE.

In some experiments, cell lysates were pre-cleared by incubation with 10 μl of rabbit serum and 40 μl of protein A-agarose. After incubation for 1 h, the slurries were centrifuged, and the supernatant recovered for immunoprecipitation of pI_{Cln} and associated proteins.

2.4. pI_{Cln} affinity assay

GST-pI_{Cln} fusion protein was generated as described above. The protein was purified by immobilization on Glutathione Sepharose 4B followed by washing with 1% Triton X-100 in PBS three times, then three times in PBS. Proteins that bind to pI_{Cln} were isolated by incubating C6 glioma cell lysates with immobilized GST-pI_{Cln} for 30 min. Unbound proteins were removed by washing five times with lysis buffer. Bound proteins were dissociated by boiling for 4 min, and then resolved by SDS-PAGE.

2.5. ^{32}P labeling of pI_{Cln}

C6 glioma cells were grown to near confluency in 100 mm diameter tissue culture plates and washed with phosphate-free MEM. Cells were depleted of phosphate by incubating them in 5 ml of phosphate-free MEM for 3 h at 37°C. The cells were then labeled with ^{32}P by incubating them for 4 h with 200 μCi/ml of ^{32}P-orthophosphoric acid.

As discussed below, protein kinase activity was present in pI_{Cln} affinity isolates and anti-pI_{Cln} immunoprecipitates. ^{32}P labeling of immunoprecipitated pI_{Cln}, immobilized GST-pI_{Cln} or other substrate proteins was carried out by incubating 10 μl of Sepharose resin, affinity isolates or immunoprecipitates with 25 μl of kinase buffer (50 mM KCl, 10 mM tris, 10 mM $MgCl_2$, pH 7.4) containing 5 μCi of ^{32}P-γ-ATP (6000 Ci/mmol) and 20 μM ATP. Unless stated otherwise, in vitro ^{32}P labeling was performed at 30°C for 15 min.

2.6. Phosphopeptide mapping and phosphoamino acid analysis

^{32}P-labeled pI_{Cln} was resolved by SDS-PAGE, transferred to a nitrocellulose membrane using a semidry transfer apparatus, and localized by autoradiography. The section of the membrane containing pI_{Cln} was cut out and digested with L-1-tosylamide-2-phenylethyl chloromethyl ketone (TPCK)-treated trypsin (Sigma, St. Louis, MO). Peptides were separated by electrophoresis in the first dimension with an ammonium bicarbonate-based buffer, pH 8.9, and by ascending chromatography in the second dimension using an isobutyric acid buffer [15]. Phosphoamino acid analysis was carried out by digesting the tryptic fragments further with 6 M HCl for 1 h at 110°C. Phosphorylated amino acids were separated by two-dimensional electrophoresis and detected by autoradiography [15].

3. Results

3.1. pI_{Cln} is phosphorylated constitutively

In order to assess the phosphorylation state of pI_{Cln} in vivo, the protein was immunoprecipitated from $^{32}PO_4$-labeled C6 glioma cells using a polyclonal rabbit anti-pI_{Cln} antiserum. As shown in Fig. 1A, pI_{Cln} is phosphorylated constitutively. Phosphoamino acid analysis revealed that the protein was phosphorylated primarily on serine residues (Fig. 1B). Exposure of C6 cells to hypotonic (150 mOsm) or hypertonic (450 mOsm) solutions for 2–5 min had no apparent effect on total ^{32}P incorporation into pI_{Cln} (data not shown).

3.2. pI_{Cln} binds to a constitutively active protein kinase

Certain protein kinases bind tightly to their substrates and can be isolated as kinase–substrate complexes [16–18]. In addition, pI_{Cln} has been shown to associate tightly and apparently selectively with several cellular proteins [2,19], including the essential myosin light chain [20]. These observations suggested that pI_{Cln} might co-immunoprecipitate with the kinase responsible for phosphorylating it. To test this possibility, C6 cell anti-pI_{Cln} immunoprecipitates were incubated with ^{32}P-ATP in kinase buffer containing phosvitin as a kinase substrate (discussed below). As shown in Fig. 2A, phosvitin was phosphorylated under these conditions. The kinase activity

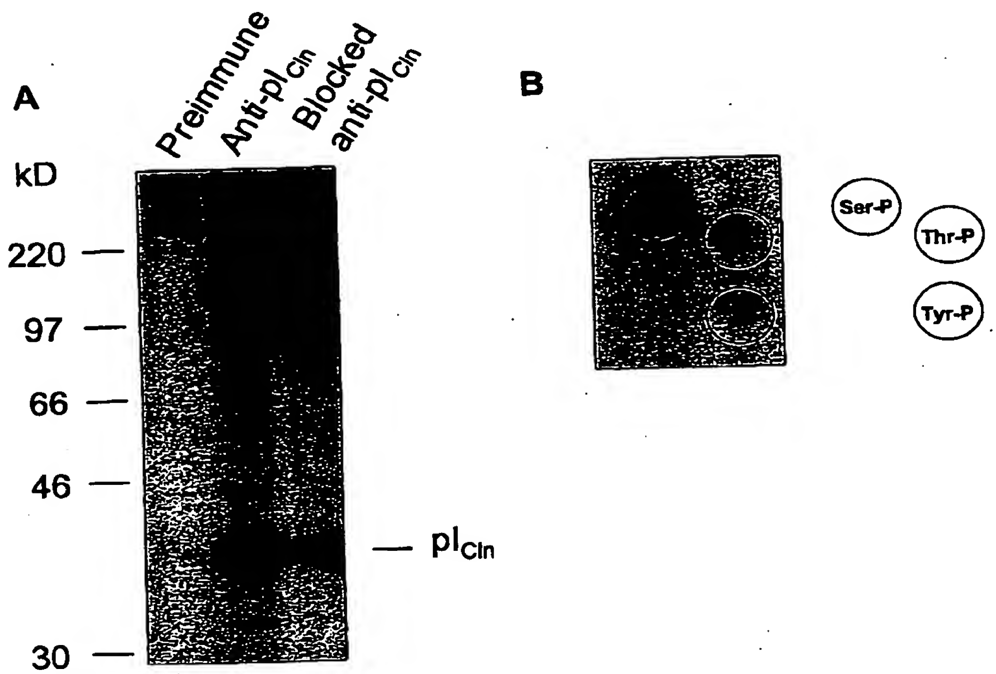

Fig. 1. pI$_{Cln}$ is a phosphoprotein. (A) C6 glioma cells were loaded with ^{32}P-orthophosphoric acid. Immunoprecipitation of pI$_{Cln}$ and associated proteins was carried out using anti-pI$_{Cln}$ polyclonal antiserum. ^{32}P-labeled proteins were resolved by SDS-PAGE and visualized by autoradiography. pI$_{Cln}$ has a predicted molecular mass of ~26 kDa [1], but appears as a ~37-kDa protein in SDS-PAGE. This anomalous electrophoretic mobility is most likely due to the large number of acidic amino acid residues present in the protein (see Fig. 7). Little or no pI$_{Cln}$ is immunoprecipitated using preimmune serum or polyclonal antiserum blocked with recombinant pI$_{Cln}$ (10 μg/μl antiserum). These experiments were repeated eight times with similar results. (B) Phosphoamino acid analysis indicates that native pI$_{Cln}$ is ^{32}P-labeled primarily on serine residues. These experiments were repeated 3 times with similar results. The three circles labeled Ser-P, Thr-P, and Tyr-P correspond to the standard positions of phosphorylated serine, threonine and tyrosine, respectively.

was not observed when C6 cells lysates were treated with anti-pI$_{Cln}$ antiserum blocked with excess recombinant pI$_{Cln}$ (data not shown) or preimmune serum (Fig. 2A).

Protein kinase activity could also be isolated using a pI$_{Cln}$ affinity assay consisting of a recombinant GST-pI$_{Cln}$ fusion protein immobilized on Sepharose–glutathione resin. C6 cell lysates were incubated with either Sepharose GST-pI$_{Cln}$ or Sepharose GST to assess the specificity of the kinase binding. After washing, ^{32}P-ATP was added to the resins in kinase buffer and incubated for 15 min. Casein was added to the reaction mixture as a kinase substrate (see below). As shown in Fig. 2B, kinase activity was detected with GST-pI$_{Cln}$, but not with GST alone. Time course studies revealed that maximum kinase activity was observed between 5 and 15 min after adding cell lysates to the affinity resins (data not shown).

The specificity of the kinase binding was assessed further by performing competition experiments. C6 cell lysates were incubated with Sepharose GST-pI$_{Cln}$ for 30 min. After washing, the resin was treated overnight with excess recombinant pI$_{Cln}$ or with BSA. ^{32}P-ATP was then added in kinase buffer and incubated for 15 min. As shown in Fig. 2C, GST-pI$_{Cln}$ was phosphorylated only in the resins treated with BSA. The ability of excess recombinant pI$_{Cln}$ to compete the kinase off of the immobilized fusion protein suggests that the interaction between the two proteins is a selective one.

Association of the kinase with pI$_{Cln}$ occurs via electrostatic interactions. The interaction between pI$_{Cln}$ and the kinase was disrupted by washing the

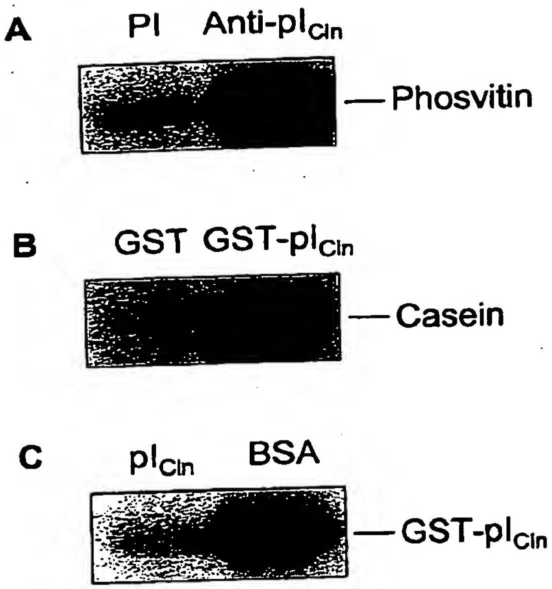

Fig. 2. A constitutively active protein kinase associates with pI$_{Cln}$. (A) pI$_{Cln}$ and associated proteins were immunoprecipitated from pre-cleared C6 glioma cell lysates using anti-pI$_{Cln}$ polyclonal antiserum. Immunoprecipitates were incubated for 15 min with 200 μCi/ml of ^{32}P-γ-ATP in kinase buffer containing 0.6 mg/ml phosvitin (used as a kinase substrate; see Fig. 4). ^{32}P-labeled phosvitin was resolved by SDS-PAGE and visualized by autoradiography. Kinase activity is observed when immunoprecipitates are isolated with anti-pI$_{Cln}$ antiserum, but not with preimmune serum. (B) A protein kinase binds selectively to recombinant pI$_{Cln}$. C6 glioma cell lysates were incubated for 30 min with immobilized GST-pI$_{Cln}$ fusion protein or immobilized GST. Affinity isolates were incubated with 200 μCi/mol of ^{32}P-γ-ATP and 0.4 mg/ml of casein (used as a kinase substrate; see Fig. 4) in kinase buffer for 15 min. Casein phosphorylation was assessed by SDS-PAGE and autoradiography. No kinase activity was isolated from C6 cell lysates incubated with GST alone. Casein is phosphorylated, however, by a protein kinase that binds to GST-pI$_{Cln}$. These experiments were repeated three times with similar results. (C) The protein kinase can be competed off GST-pI$_{Cln}$ by excess recombinant pI$_{Cln}$, but not by bovine serum albumin (BSA). C6 glioma cell lysates were incubated for 30 min with immobilized GST-pI$_{Cln}$ fusion protein. After washing, the affinity isolates were incubated overnight with BSA or recombinant pI$_{Cln}$ added to a final concentration of 1 mg/ml. The affinity isolates were then washed and incubated for 15 min with 200 μCi/ml of ^{32}P-γ-ATP in kinase buffer. Phosphorylation of GST-pI$_{Cln}$ was assessed by SDS-PAGE and autoradiography. These experiments were repeated three times with similar results.

affinity resins with increasing concentrations of NaCl. At concentrations above 200 mM, kinase activity was undetectable (data not shown). This observation suggests an important role for charged amino acid domains in mediating kinase binding.

pI$_{Cln}$ contains two clusters of negatively charged amino acids. We refer to these regions as acidic domains 1 and 2 (AD1 and AD2; see Fig. 7). We postulated that these regions might be important for kinase binding, given the fact that kinase binding was sensitive to the salt concentration in the washing buffer. To test this possibility, we generated the following truncated forms of GST-pI$_{Cln}$: M1-H241 (full length), M1-S100, M1-Y156, D101-Y156, D101-H241, V158-H241. AD1 and AD2 are located between D101 and Y156. The ability of the truncated pI$_{Cln}$ molecules to bind the kinase was assessed by performing the affinity and kinase assays described above. GST-pI$_{Cln}$ was used as a kinase substrate. As shown in Fig. 3A, no kinase binding was detected on M1-S100 or V158-H241. These two fragments lack AD1 and AD2. Kinase activity was detected, however, on M1-Y156 and D101-H241, which contain both acidic domains. D101-Y156, which is the smallest pI$_{Cln}$ fragment containing both AD1 and AD2, was also capable of binding the kinase. These results suggest that AD1 and/or AD2 may be important for binding the kinase directly. Alternatively, separate kinase binding protein(s) may interact with AD1 and AD2.

We also assessed the ability of the kinase to phosphorylate various truncated pI$_{Cln}$ molecules. Affinity and kinase assays were performed as described above. As shown in Fig. 3B, the four truncated constructs that bound the kinase were also phosphorylated by it.

3.3. Characteristics of the pI$_{Cln}$-associated kinase

Phosphoamino acid analysis was performed on recombinant pI$_{Cln}$ phosphorylated by the pI$_{Cln}$-associated kinase isolated with either affinity assay or immunoprecipitation. The pI$_{Cln}$-associated kinase phosphorylated pI$_{Cln}$ on serine residues only (data not shown), indicating that it is a serine–threonine protein kinase.

The pI$_{Cln}$-associated kinase had a broad substrate specificity and was capable of phosphorylating acidic proteins such as casein, α-casein and phosvitin, as well as myelin basic protein (MBP) (Fig. 4). Minor phosphorylation of β-casein was also observed. The

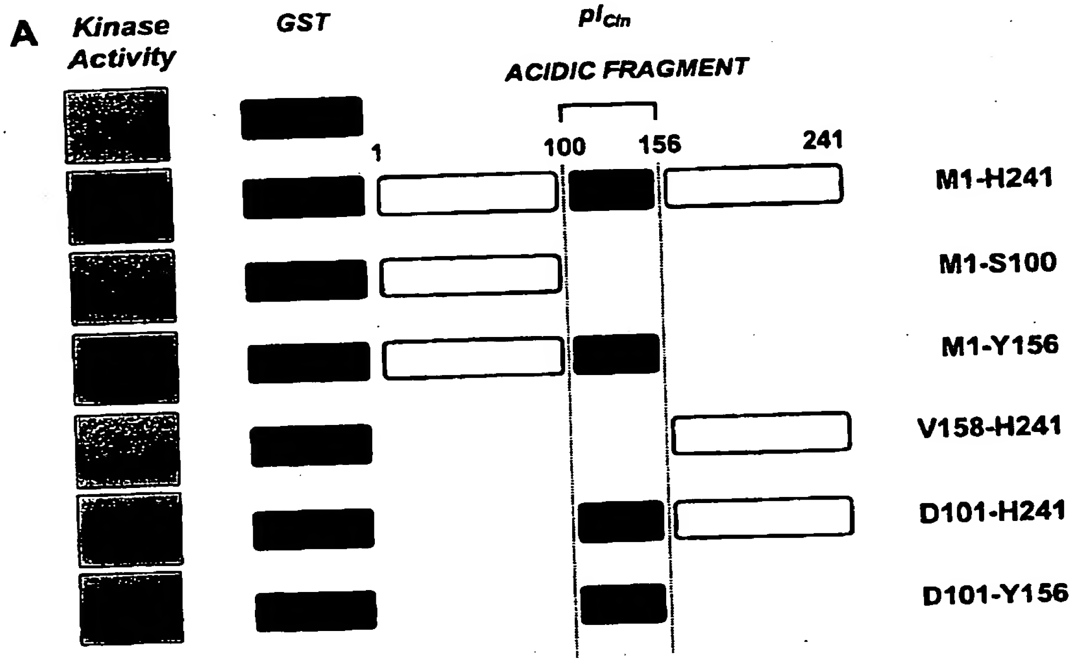

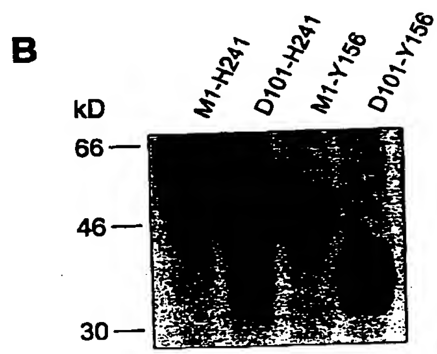

Fig. 3. Binding of the pI_{Cln}-associated kinase to truncated forms of pI_{Cln}. (A) Acidic amino acid domains mediate pI_{Cln}-kinase binding. pI_{Cln} deletion mutants were prepared as GST fusion proteins and immobilized on Glutathione Sepharose resin as described for full-length pI_{Cln} in Section 2. Constructs were exposed to rat C6 cell lysates for 30 min and then washed five times with lysis buffer and two times with kinase buffer. Bound kinase was eluted by washing with 200 mM NaCl in kinase buffer. Kinase activity was assessed by incubating 25 μl of each eluate with 5 μCi of ^{32}P-γ-ATP and 50 μg of immobilized full length GST-pI_{Cln} for 15 min. ^{32}P-labeled pI_{Cln} was resolved by SDS-PAGE and visualized by autoradiography. Kinase binding activity was observed only with those constructs bearing the acidic fragment, D101-D156, which contains both AD1 and AD2 (see Fig. 7). Experiments were repeated two times with similar results. (B) Phosphorylation of pI_{Cln} occurs close to the kinase binding site. The pI_{Cln}-associated kinase was isolated using one of the four truncated constructs shown. Kinase activity was assessed using each truncated GST-pI_{Cln} construct as a kinase substrate.

basic protein protamine was not phosphorylated by the pI_{Cln}-associated kinase.

Most protein kinases require the presence of Mg^{2+} for full activity. As shown in Fig. 5A, pI_{Cln}-associated kinase activity was increased in a concentration dependent manner by Mg^{2+}. Kinase activity was reduced greatly when 10 mM Mg^{2+} was replaced with 10 mM Mn^{2+} or 10 mM Co^{2+}. No kinase activity was detectable when 10 mM Ca^{2+} replaced Mg^{2+} (Fig. 5A).

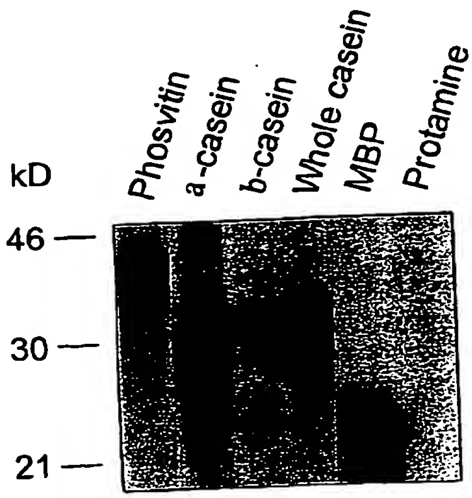

4. The pI_{Cln}-associated kinase has broad substrate speci-
y. Kinase activity was isolated by affinity assay. The kinase
; then eluted from the affinity isolates by incubating for 15
ı in kinase buffer containing 200 mM NaCl. Substrate speci-
ty was assessed by adding to the supernatant 200 μCi/ml of
-γ-ATP and 0.4 mg/ml of various substrate proteins. After a
min incubation, the proteins were resolved and visualized by
S-PAGE and autoradiography. This experiment was repeated
ee times with identical results. A similar substrate specificity
s observed when kinase activity was isolated by immuno-
:cipitation (data not shown).

pI_{Cln} has consensus sequences for phosphorylation / protein kinase A, C and G, and casein kinase I and (CKI and CKII) [21,22]. Y151 and Y156 may also be potential sites for phosphorylation by tyrosine kinases [23,24] (see Fig. 7). Of these kinases, only CKI and CKII are in general constitutively active. In addition, CKI and CKII preferentially phosphorylate acidic proteins [25], and they have frequently been isolated by co-immunoprecipitation with their substrates [16–18]. We, therefore, examined the sensitivity of the pI_{Cln}-associated kinase to heparin, zinc and 5,6-dichloro-1-β-D-ribofuranosylbenzimidazole (DRB), which are known inhibitors of CKI and CKII [26–29]. As shown in Fig. 5B, all three drugs inhib-

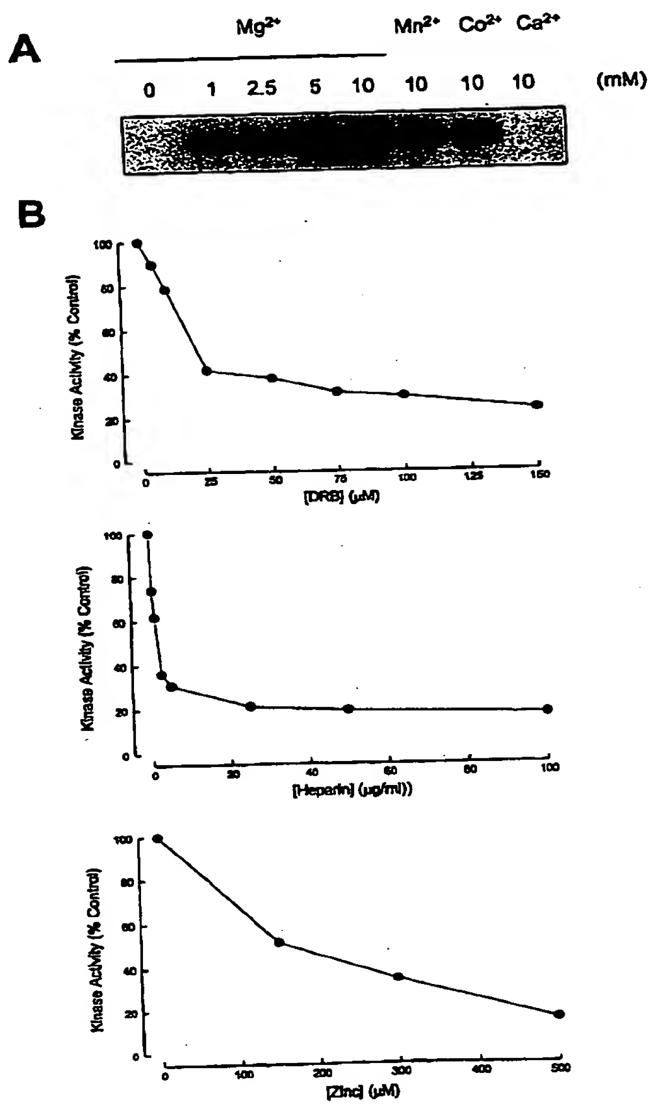

ig. 5. Pharmacological characteristics of the pICln-associated
ınase. (A) Kinase activity requires the presence of Mg^{2+}.
I_{Cln}-associated kinase activity was isolated by affinity assay.
ffinity isolates were incubated for 15 min in kinase buffer
ontaining 200 μCi/ml of ^{32}P-γ-ATP and various concentra-
ons of divalent cations. Phosphorylation of GST-pI_{Cln} was
ssessed by SDS-PAGE and autoradiography. Divalent cations
upported kinase activity with the following potency: $Mg^{2+} \gg$
$Co^{2+} > Mn^{2+} \gg Ca^{2+}$. This experiment was repeated two times
vith similar results. (B) The pI_{Cln}-associated kinase is inhibited
by CKI and CKII inhibitors. Kinase activity was isolated by
affinity assay, and affinity isolates were incubated for 15 min in
kinase buffer containing 200 μCi/ml of ^{32}P-γ-ATP and various
concentrations of DRB, heparin or zinc. Proteins were resolved
by SDS-PAGE and visualized by Coomassie staining of the gel.
The protein band corresponding to GST-pI_{Cln} was cut out of the
gel and the radioactivity quantified by Cerenkov counting. Results are expressed as percent of the control. A similar inhibitor sensitivity was observed with kinase activity isolated by immunoprecipitation (data not shown).

ited kinase activity in a concentration-dependent manner. The maximal inhibition observed for each drug was approximately 80%.

The inhibitor sensitivity of the pI_{Cln}-associated kinase suggested that it may be either CKI or CKII. To address this possibility directly, we performed Western blot analysis of the pI_{Cln}-associated kinase isolated by affinity assay using anti-CKI or anti-CKII antibodies.

Mammalian cells possess at least four isoforms of CKI [30]. Casein kinase II is composed of three subunits referred to as α, α' and β [25]. To assess whether CKI and CKII are expressed in C6 cells, lysates from $\sim 2 \times 10^7$ cells (half of a 10 cm diameter culture dish) were prepared in 1 ml of lysis buffer. Twenty-five microliters of this material were then subjected to Western analysis using antibodies to the conserved CKI kinase domain (kindly provided by Dr. David Virshup, University of Utah [31]) and antibodies to the α, α' and β subunits of CKII (kindly provided by Dr. David Litchfield, Manitoba Institute of Cell Biology [32]). Anti-CKI antibodies recognized 2 proteins in C6 cell lysates (data not shown). Antibodies to the α, α' and β subunits of CKII each reacted with proteins of the appropriate molecular mass (data not shown).

To determine if CKI or CKII interact with pI_{Cln}, C6 cell lysates were subjected to GST-pI_{Cln} affinity purification as described previously. The amount of kinase isolated was maximized by preparing lysates from cells grown on ten 10-cm diameter culture dishes ($\sim 40 \times 10^7$ cells). Affinity-isolated proteins were resolved by SDS-PAGE and subjected to anti-CKI or CKII Western analysis. No proteins were detected (data not shown) even when exposure times were 20-fold longer than those used for Western analysis of total cell lysates. These findings suggest that the CKI or CKII are not the kinases that bind to and phosphorylate pI_{Cln} in vitro.

3.4. Phosphopeptide mapping

Native pI_{Cln} was phosphorylated by incubating C6 glioma cells with ^{32}P-orthophosphoric acid, and the protein was isolated by immunoprecipitation and subjected to trypsin digestion as described in Section 2.

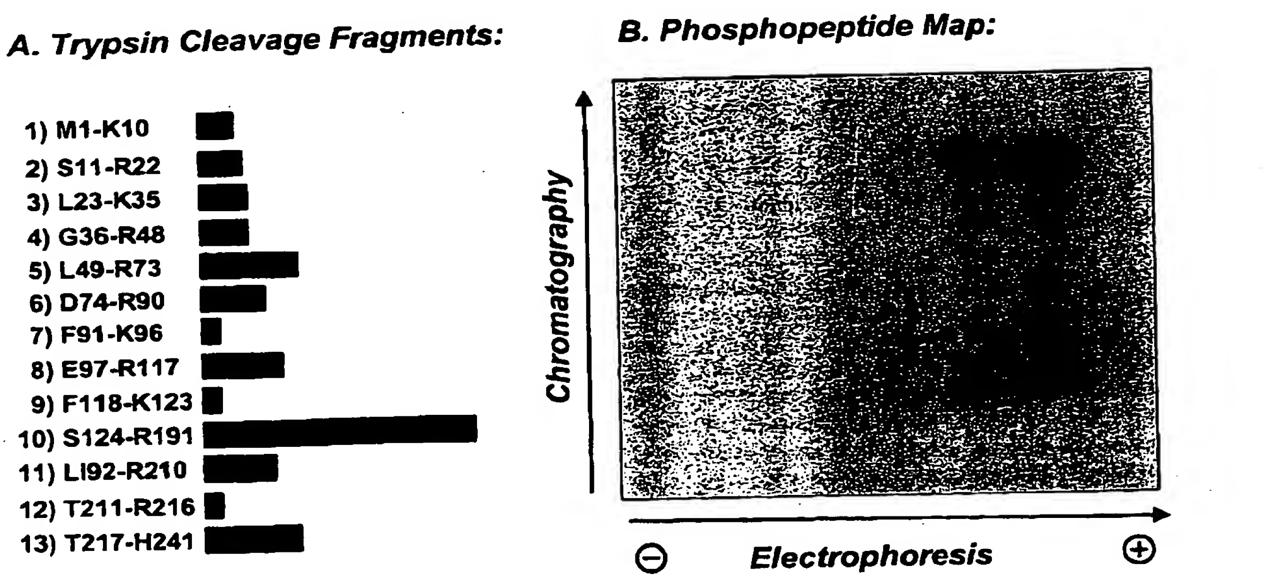

Fig. 6. Phosphopeptide map of native pI_{Cln}. pI_{Cln} was immunoprecipitated from ^{32}P-orthophosphoric acid loaded C6 glioma cells. Proteins were separated by SDS-PAGE, blotted onto nitrocellulose membranes and digested with trypsin. (A) Predicted trypsin cleavage fragments of rat pI_{Cln}. Fragments 8 and 10 (solid bars) contain large numbers of acidic amino acid residues, as well as serine residues that are likely sites of phosphorylation. (B) Phosphopeptide map. Trypsin cleavage fragments were separated by electrophoresis and ascending chromatography using thin layer chromatography plates. Phosphopeptides were visualized by autoradiography.

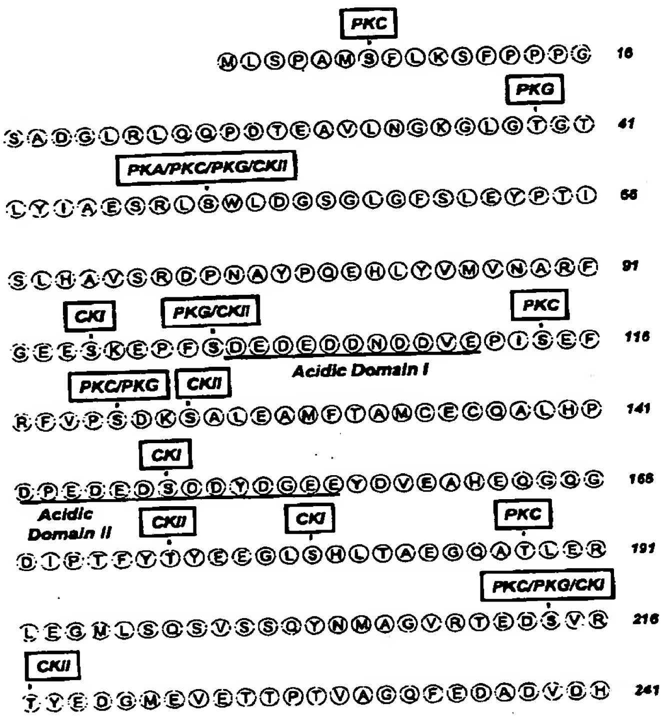

Fig. 7. Amino acid sequence of pI_{Cln} cloned from rat C6 glioma cells. Consensus sites for phosphorylation by protein kinase A (PKA), protein kinase C (PKC), protein kinase G (PKG), casein kinase I (CKI) and casein kinase II (CKII) were identified using data published by Pearson and Kemp [21] and Kennelley and Krebs [22]. Serine and threonine residues that can putatively be phosphorylated by these kinases are highlighted in bold. The consensus sequences considered were as follows: PKA, R-X-S* [21]; PKC, S*/T*-$X_{2\text{-}0}$-R/$K_{1\text{-}3}$ [22] or K/R-X-S*/T* [21]; PKG, R/K-X-S*/T* or R/K-X-X-X-S*T* [21]; CKI, D/$E_{2\text{-}4}$-$X_{2\text{-}0}$-S*/T* [22]; CKII, S*/T*-X-X-E/D-X [21], where X denotes any amino acid and the asterisks denote phosphorylated serine and threonine residues. The amino acid sequence located on the N-terminal side of Y151 and Y156 is highly acidic and enriched in glutamate and aspartate residues. This suggests that these tyrosine residues may be sites of phosphorylation by tyrosine kinases [23,24]. Acidic amino acid domains (AD1 and AD2) are underlined.

In our initial attempts to separate pI_{Cln} phosphopeptides, we used a formic acid/acetic acid pH 1.9 electrophoresis buffer. For the chromatography phase of the separation, we used a so-called phospho-chromatography buffer [15]. With this buffer system, the phosphopeptides did not separate and remained at the origin. Subsequently, we used a pH 8.9 ammonium bicarbonate electrophoresis buffer and an isobutyric acid chromatography buffer designed to separate extremely hydrophilic peptides [15]. We obtained good separation of two phosphopeptides with this buffer system (Fig. 6). These results indicate that there are at least two phosphorylated serine residues on pI_{Cln}. The buffer system required to separate the pI_{Cln} phosphopeptides indicates that phosphorylated serines are located on acidic trypsin cleavage fragments.

4. Discussion

VSOAC is an outwardly rectifying, swelling-activated anion channel responsible for volume regulatory Cl^- and organic solute transport [6,7]. pI_{Cln} has been suggested to be VSOAC [8,9] or a VSOAC regulator [2]. More recently, it has been suggested that pI_{Cln} activates in a non-selective manner a channel that is distinct from VSOAC [10,11]. The controversy raised over pI_{Cln} is reminiscent of those surrounding the function of min K and phospholemman [33,34]. These controversies have raised fundamental questions about ion channel structure, ion channel regulators and proteins that indirectly modify ion channel function. Resolution of the pI_{Cln} controversy will require extensive molecular and cellular characterization of this protein using a variety of approaches, including planar lipid bilayer reconstitution. Our goal in the present investigation was to further define the general biochemical properties of pI_{Cln}, specifically its phosphorylation state. pI_{Cln} contains a number of consensus sites for phosphorylation by CKI, CKII, protein kinases (PK) A, C, and G and possibly tyrosine kinases (see Fig. 7), suggesting that phosphorylation may control the functional properties of the protein.

As shown in Fig. 1, pI_{Cln} is constitutively phosphorylated, primarily on serine residues. Immunoprecipitation and affinity assay studies revealed that pI_{Cln} associates in an apparently selective fashion with a serine/threonine kinase (Fig. 2). This kinase is constitutively active, has broad substrate specificity (Fig. 4), and is inhibited in a concentration-dependent manner by zinc, DRB and heparin (Fig. 5).

The identity of the pI_{Cln}-associated kinase is unknown. Of all the known kinases for which there are consensus phosphorylation sites on pI_{Cln}, three can be ruled out as possible candidates: tyrosine kinases,

CKI and CKII (see Fig. 7). PKC or PKG are probably not involved in the in vitro phosphorylation of pI_{Cln}. These kinases require activation by phorbol esters or cGMP, which are not present in our assay buffer. PKA is also unlikely to be important. In general, PKA requires activation by cAMP, but at least one report suggests that it can be constitutively active in vitro [35]. We observed, however, that the Walsh peptide (New England Biolabs, Beverly, MA), a highly specific and potent PKA inhibitor [36], had no effect on pI_{Cln}-associated kinase activity (unpublished observations). Given these findings, it is likely that the pI_{Cln}-associated kinase is either a new kinase or a kinase for which the consensus phosphorylation sites have not been described and/or cataloged.

Proteins with apparent molecular masses of 17, 29, 72, and 160 kDa bind in what seems to be a selective fashion to pI_{Cln} [19,20] (see also Ref. [2]). Microsequencing has revealed that p17 is the essential myosin light chain [20]. Krapivinsky et al. [2] have also concluded that actin binds selectively to pI_{Cln}. The identities of the other pI_{Cln} binding proteins are presently unknown. It is possible that one of these proteins is the pI_{Cln}-associated kinase. In gel kinase, assays may provide a means to test this idea directly.

We do not know yet whether the kinase isolated in vitro is the same one responsible for phosphorylating pI_{Cln} in intact cells. We attempted to address this issue by performing phosphopeptide mapping on pI_{Cln} immunoprecipitated from C6 glioma cells, GST-pI_{Cln} or recombinant pI_{Cln} cleaved from the GST moiety. These three proteins were phosphorylated using the kinase isolated by anti-pI_{Cln} immunoprecipitation. In all cases, separation of the phosphopeptides required a buffer system optimized for acidic proteins. This suggests that the pI_{Cln}-associated kinase phosphorylates serine residues located on acidic trypsin cleavage fragments similar to that observed for pI_{Cln} phosphorylated in vivo (see Section 3). Each of the three substrate proteins, however, yielded a unique phosphopeptide map (data not shown). These maps were distinct from the map obtained with native pI_{Cln}. One interpretation of these results is that the kinase observed in vitro is distinct from the kinase that phosphorylates pI_{Cln} in intact cells. It is equally likely, however, that the state of the protein (i.e., bound to antibody, linked to GST or free) and/or the activity of other kinases and phosphatases may influence the overall phosphorylation state of pI_{Cln} in vivo. Additional studies are required to assess the physiological role played by the pI_{Cln}-associated kinase in phosphorylating the protein in vivo.

Phosphopeptide mapping provided insight into the location of phosphorylated serine residues on pI_{Cln}. Rat pI_{Cln} contains 12 predicted trypsin cleavage sites and yields 13 fragments upon trypsin cleavage (Fig. 6). As discussed above, the pI_{Cln} phosphopeptides we isolated appeared to be highly acidic. Of the 13 trypsin cleavage fragments, three contain large numbers of acidic amino acids: E97-R117 (11 Glu and Asp residues), S124-R191 (20 Glu and Asp residues) and T217-H241 (8 Glu and Asp residues). There are no serine residues on T217-H241. In contrast, there are two serine residues in E97-R117 and three in S124-R191. These findings suggest that S100, S114, S124, S148 and/or S179 are the most likely sites for phosphorylation of rat pI_{Cln} in vivo. Other phosphorylation sites may exist as well. Mutagenesis studies are required to directly determine the sites of phosphorylation.

The putative location of phosphorylated serine residues on acidic peptide fragments is consistent with other observations. As noted in Section 3, association of the kinase with pI_{Cln} is sensitive to the salt concentration of the washing buffer, suggesting an important role for charged amino acid domains in mediating kinase binding. The pI_{Cln} truncation experiments shown in Fig. 3A support this idea. The kinase binds only to pI_{Cln} fragments containing AD1 and AD2. Furthermore, D101-Y156, a 56 amino acid fragment containing both AD1 and AD2, is sufficient for kinase binding. Our results suggest that the kinase binds directly or indirectly via accessory proteins to AD1 and/or AD2 and phosphorylates nearby serine residues. This conclusion is supported by the observation that pI_{Cln} truncation fragments containing AD1 and AD2 were not only capable of binding the kinase, but were also phosphorylated by it (Fig. 3B).

Clusters of acidic amino acid residues have been shown to be important for several other protein–protein interactions. These include the interaction of eukaryotic transcription factors with components of the transcription machinery [37,38], and the binding of transported proteins to the protein transport system located in the mitochondrial outer membrane [39]. A cluster of acidic amino acid residues on the mam-

nalian endopeptidase furin is thought to be important for internalization of the protein from the plasma membrane and localization to the trans-Golgi network [40].

The physiological role of pI_{Cln} phosphorylation is unknown. If pI_{Cln} is the VSOAC channel or a VSOAC regulator, as suggested by Krapivinsky et al. [2] and Gschwentner et al. [8,9], then phosphorylation may control channel activity. In some cell types, phosphorylation and dephosphorylation events have been suggested to play a role in controlling regulatory volume decrease and the activity of volume-sensitive anion channels [41–44]. At least one recent study has suggested that phosphorylation may control swelling-induced activation of VSOAC [45]. In addition, stimulation of PKA or PKC with cAMP and phorbol esters has been shown to enhance VSOAC activity [14,46].

Recent findings of Voets et al. [11,47] and Buyse et al. [10] have challenged the proposed connection between VSOAC and pI_{Cln}. These investigators observed that I_{Cln} was induced in oocytes by overexpression of either pI_{Cln} or the unrelated protein ClC-6. Careful examination of I_{Cln} demonstrated that its characteristics were distinct from those of the endogenous swelling-activated VSOAC current described in oocytes [10–13]. Furthermore, Buyse et al. [10] and our laboratory (Strange et al., unpublished observations) have observed that oocytes possess an endogenous, constitutively active conductance that has the same characteristics as the current proposed by Paulmichl et al. [1] to arise from expression of a mutant form of pI_{Cln}. Voets et al. [47] recently attempted to reproduce the mutagenesis studies of Paulmichl et al. [1]. They observed that expression of the so-called AAA mutant induced a current identical to that of wild type pI_{Cln}. When taken together, these results have led Buyse et al. [10] and Voets et al. [47] to conclude that expression of pI_{Cln} in oocytes turns on an endogenous anion current that is distinct from VSOAC.

From the above discussion, it is clear that the function of pI_{Cln} remains obscure. Identification of the pI_{Cln}-associated kinase, determination of the physiological consequences of pI_{Cln} phosphorylation, and assessment of the effect of phosphorylation on channel activity induced by pI_{Cln} in planar lipid bilayers may provide insight into the physiological role of this protein.

Acknowledgements

This work was supported by NIH grants NS30591 and DK51610 and by an Established Investigator Award from the American Heart Association to K. Strange.

References

[1] M. Paulmichl, Y. Li, K. Wickman, M. Ackerman, E. Peralta, D. Clapham, Nature 356 (1992) 238–241.
[2] G.B. Krapivinsky, M.J. Ackerman, E.A. Gordon, L.D. Krapivinsky, D.E. Clapham, Cell 76 (1994) 439–448.
[3] H. Okada, I. Kuniaki, K. Nunoki, N. Taira, Biochim. Biophys. Acta 1234 (1995) 145–148.
[4] K. Ishibashi, S. Sasaki, S. Uchida, T. Imai, F. Marumo, Biochem. Biophys. Res. Commun. 192 (1993) 561–567.
[5] A. Schmarda, U.O. Nagl, M. Gschwentner, J. Furst, S. Hofer, P. Deetjen, M. Paulmich, Cell. Physiol. Biochem. 7 (1997) 298–302.
[6] K. Strange, P.S. Jackson, Kidney Int. 48 (1995) 994–1003.
[7] K. Strange, F. Emma, P.S. Jackson, Am. J. Physiol. 270 (1996) C711–C730.
[8] M. Gschwentner, U.O. Nagl, E. Woll, A. Schmarda, M. Ritter, M. Paulmich, Pflugers Arch. 430 (1995) 464–470.
[9] M. Gschwentner, A. Susanna, A. Schmarda, A. Laich, U.O. Nagl, H. Ellemunter, P. Deetjen, J. Frick, M. Paulmichl, J. Allergy Clin. Immunol. 98 (1996) S98–S101.
[10] G. Buyse, T. Voets, J. Tytgat, C. De Greef, G. Droogmans, B. Nilius, J. Eggermont, J. Biol. Chem. 272 (1997) 3615–3621.
[11] T. Voets, G. Buyse, J. Tytgat, G. Droogmans, J. Eggermont, B. Nilius, J. Physiol. 495 (1996) 441–447.
[12] M.J. Ackerman, K.D. Wickman, D.E. Clapham, J. Gen. Physiol. 103 (1994) 153–179.
[13] M. Hand, R. Morrison, K. Strange, J. Membr. Biol. 157 (1997) 9–16.
[14] P.S. Jackson, K. Strange, Am. J. Physiol. 265 (1993) C1489–C1500.
[15] W.J. Boyle, P. van der Geer, T. Hunter, Methods Enzymol. 201 (1991) 110–149.
[16] O. Filhol, J. Baudier, C. Delphin, P. Loue-Mackenbach, E.M. Chambaz, C. Cochet, J. Biol. Chem. 267 (1992) 20577–20583.
[17] M.K. Bennett, K.G. Miller, R.H. Scheller, J. Neurosci. 13 (1993) 1701–1707.
[18] Y. Miyata, I. Yahara, J. Biol. Chem. 267 (1992) 7042–7047.
[19] F. Emma, R. Sanchez-Olea, K. Strange, J. Gen. Physiol. 108 (1996) 23a, (abstract).
[20] R. Sanchez-Olea, M. Coghlan, K. Strange, Biophys. J. 72 (1997) A5, (abstract).
[21] R.B. Pearson, B.E. Kemp, Methods Enzymol. 200 (1991) 62–81.

[22] P.J. Kennelly, E.G. Krebs, J. Biol. Chem. 266 (1991) 15555–15558.
[23] Z. Songyang, K.L. Carraway III, M.J. Eck, S.C. Harrison, R.A. Feldman, M. Mohammadi, J. Schlessinger, S.R. Hubbard, D.P. Smith, C. Eng, M.J. Lorenzo, B.A.J. Ponder, B.J. Mayer, L.C. Cantley, Nature 373 (1995) 536–539.
[24] D.A. Tinker, J.L. Cartron, J.S. McMurray, V.A. Levin, Anticancer Res. 12 (1992) 123–128.
[25] J.E. Allende, C.C. Allende, FASEB J. 9 (1995) 313–323.
[26] G.M. Hathaway, T.H. Lubben, J.A. Traugh, J. Biol. Chem. 255 (1980) 8038–8041.
[27] M. Gatica, M.V. Hinrichs, A. Jedlicki, C.C. Allende, J.E. Allende, FEBS Lett. 315 (1993) 173–177.
[28] R. Zandomeni, M.C. Zandomeni, D. Shugar, R. Weinmann, J. Biol. Chem. 261 (1986) 3414–3419.
[29] S.D. Gross, D.P. Hoffman, P.L. Fisette, P. Baas, R.A. Anderson, J. Cell Biol. 130 (1995) 711–724.
[30] J. Rowles, C. Slaughter, C. Moomaw, J. Hsu, M.H. Cobb, Proc. Natl. Acad. Sci. U.S.A. 88 (1991) 9548–9552.
[31] K.J. Fish, A. Cegielska, M.E. Getman, G.M. Landes, D.M. Virshup, J. Biol. Chem. 270 (1995) 14875–14883.
[32] D.W. Litchfield, F.J. Lozeman, M.F. Cicirelli, M. Harrylock, L.H. Ericsson, C.J. Piening, E.G. Krebs, J. Biol. Chem. 266 (1991) 20380–20389.
[33] T. Tzounopoulos, J. Maylie, J.P. Adelman, Biophys. J. 69 (1995) 904–908.
[34] K. Shimbo, D.L. Brassard, R.A. Lamb, L.H. Pinto, Biophys. J. 69 (1995) 1819–1829.
[35] I. Izawa, N. Tamaki, H. Saya, FEBS Lett. 382 (1996) 53–59.
[36] D.A. Walsh, C.D. Ashby, C. Gonzalez, D. Calkins, E.H. Fischer, E.G. Krebs, J. Biol. Chem. 246 (1971) 1977–1985.
[37] M. Ptashne, Nature 355 (1988) 683–689.
[38] R. Li, M.R. Botchan, Cell 73 (1993) 1207–1221.
[39] L. Bolliger, T. Junne, G. Schatz, T. Lithgow, EMBO J. 14 (1995) 6318–6326.
[40] P. Voorhees, E. Deignan, E.V. Donselaar, J. Humphrey, M.S. Marks, P.J. Peters, J.S. Bonifacino, EMBO J. 14 (1995) 4961–4975.
[41] L. Robson, M. Hunter, J. Physiol. 480 (1994) 1–7.
[42] B.C. Tilly, N. van den Berghe, L.G.J. Tertoolen, M.J. Edixhoven, H.R. de Jonge, J. Biol. Chem. 268 (1993) 19919–19922.
[43] J.W. Lohr, L.A. Yohe, Brain Res. 667 (1994) 263–268.
[44] M. Villaz, J.C. Cinniger, W.J. Moody, J. Physiol. 488 (1995) 689–699.
[45] K. Meyer, C. Korbmacher, J. Gen. Physiol. 108 (1996) 177–193.
[46] K. Strange, R. Morrison, L. Shrode, R. Putnam, Am. J. Physiol. 265 (1993) C244–C256.
[47] T. Voets, G. Buyse, G. Droogmans, J. Eggermont, B. Nilius, J. Physiol. 506 (1998) 47P (abstract).